Dear Editor,

We would like to thank all the reviewers for their constructive comments. The insightful suggestions have been fully considered in the revised manuscript. Point-by-point responses to the suggestions, corresponding updates with the revised manuscript, and the finalized version have been uploaded.

In the following, original suggestions, our response, and updates on the revised manuscript are shown in **bold**, normal, and *italic*, respectively.

Kind Regards,

Jing Chen, Yuhang Hao, and Peizhao Li

Anonymous Referee #2

General comments:

The authors present simultaneous measurements of particle number size distributions, aerosol optical and hygroscopic properties, and bulk chemical composition from urban Chongqing during the extremely hot summer of 2022 to investigate the characteristics of new particle formation (NPF) events for two distinct cases: polluted and clean-heatwave event. The authors claim that heatwave(s) may induce stronger photooxidation, enhancing hygroscopic growth and thereby aerosol direct radiative forcing. Overall, the manuscript is well-written. Although the objective of this study is intriguing, I find that a single heatwave event or unusually hot summer is not necessarily sufficient to support the findings and therefore speculation or tall statements must be avoided. I would like to recommend the publication of this study after the authors carefully address all the following concerns.

Response: We thank the reviewer for the insightful comments and supportive recommendation on this manuscript.

Specific comments:

RC1. Fig. 1c shows the time evolution of (hourly?) temperature during the study period. Air temperature (RH) steadily increased (decreased) after 8 Aug. Surprisingly, the wind speed is slightly higher during period P2 (heatwave. Fig 2i), but heatwaves are usually associated with stagnant conditions. Nairn et al. (2015) calculated the excess heat factor to identify heatwave events. Could this be explored to determine the spatial extent of this particular heatwave event, using gridded temperature data if it is available for the region? Heatwaves are anomalous events characterized by extremely high surface air temperatures, typically lasting over a week. A mere surface air temperature threshold is not the best indicator of a regional heatwave event. This is indeed critical in the content of regional NPF events and the conclusions drawn from this study. The question is — Did the heatwave event trigger the NPF event, or did relatively cleaner conditions favour the NPF event or specific dynamical weather pattern favoured NPF (high-pressure system) or a combination of everything?

Response: Figure 1c depicts the temporal variation of hourly temperature records during the study period. Although slightly higher than that of P1 (Table S2), the mean level of wind speed during P2 is still within 2.0 m/s, i.e., the gentle breeze condition. The 2022 summer in China was demonstrated to be characterized by an unprecedented heatwave event, as evidenced by regional gridded temperature results from recent studies (Chen et al., 2024; Wang et al., 2024). These studies have illustrated the widespread distribution of elevated temperature levels across multiple regions in China during August 2022 compared to the same periods in previous years, with particularly intense heatwave impacts observed in Southwest China. This robust evidence confirms that our study period was indeed influenced by a severe and extensive heatwave event.

Following the reviewer's suggestion, we have calculated the corresponding Excess Heat Factor (EHF) metric (Nairn and Fawcett, 2014) for the study period (Figure R1). The EHF results suggest that the period following 9 August 2022 belongs to heatwave cases, aligning with the observed meteorological conditions. In addition

to the EHF analysis, China Meteorological Administration normally defines heatwaves as follows: three or more consecutive days with a daily maximum temperature, T_{max} , exceeding 35 °C (http://www.cmastd.cn/standardView.jspx?id=2103) (Guo et al., 2016; Sun et al., 2014; Tan et al., 2007). According to the above criteria and the consistently occurrence of $T_{max} \geq 38$ °C (approximately the last 25th percentile of temperature records for the whole observation period, Figure R1a-b), 7–19 August 2022 was classified as a heatwave-dominated period in this study.

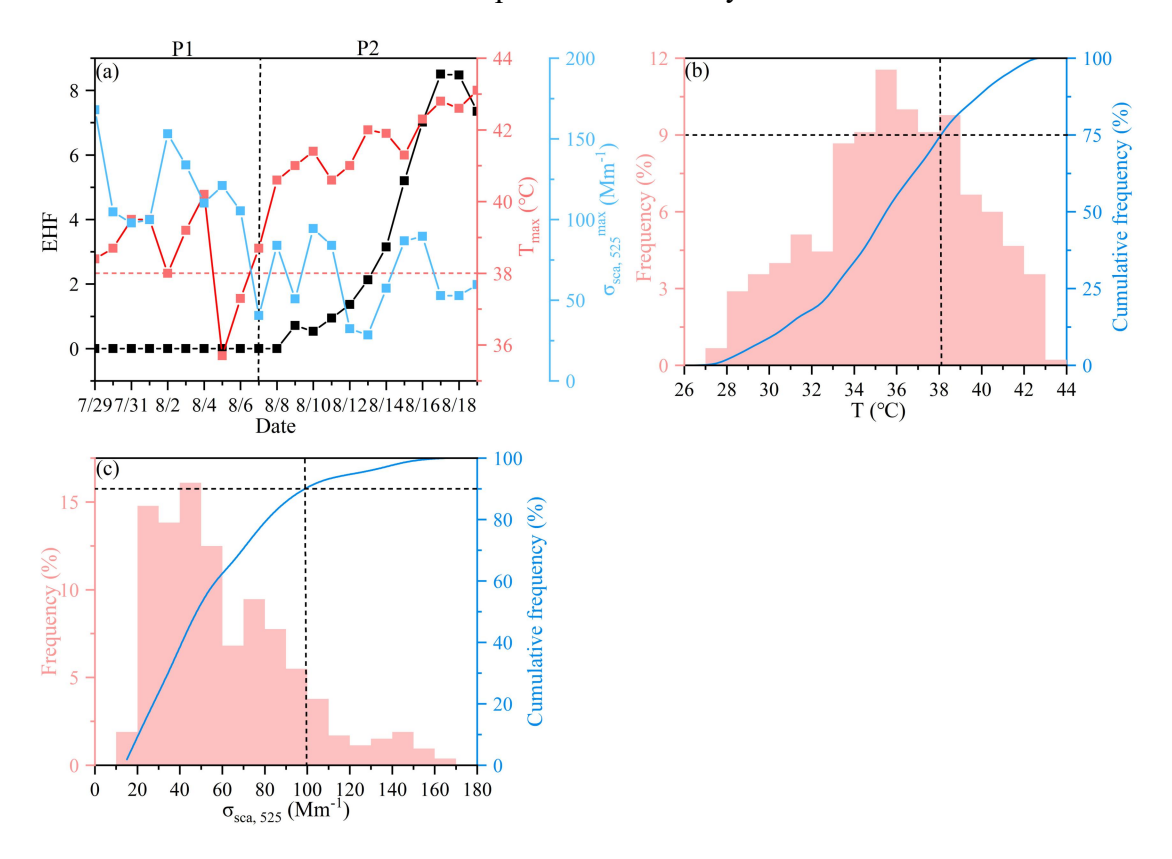


Figure R1. (a) Time series of calculated EHF, along with the daily maximum temperature (T_{max}) and dry $\sigma_{sca, 525}$ results, during the study period. The corresponding occurrence frequency and cumulative frequency of hourly (b) temperature and (c) $\sigma_{sca, 525}$ data records.

On the other hand, we agree that NPF events during different periods are not solely influenced by temperature/solar radiation variations but also regulated by other factors (e.g., pollution levels). The environment was significantly cleaner after August 6, as evidenced by the fact that the hourly mean $\sigma_{sca, 525}$ values were exclusively below

100 Mm⁻¹ (approximately the last 10th percentile of dry aerosol light scattering data, regarded as the threshold value of relatively polluted cases; Figure R1c). In this sense, we defined the period from July 29 to August 6 as a relatively polluted hot period (P1; NPF during this period was marked as NPF_p), whereas a clean and heatwave-dominated period from August 7-19 (P2; NPF was accordingly labelled as NPF_{C, HW}). This dual consideration of temperature and pollution levels could provide a more holistic understanding of the mechanisms of NPF events and related environmental and climatic impacts. To avoid arbitrary statements, we emphasize that heatwave-induced atmospheric conditions diverge significantly from that of normal periods, as characterized by the observed higher (lower) solar radiation (RH), along with the potential changes in types and concentrations of gaseous precursors in this study.

Accordingly, we have revised the manuscript to underscore the distinct changes in NPF events and aerosol optical hygroscopicity against the background of heatwaves, thereby deepening insights into the implications of heatwave conditions for aerosol physicochemical properties.

Updated on the manuscript:

Abstract: Compared to the NPF_P events, $NPF_{C, HW}$ occurred approximately one hour earlier and the subsequent growth was prolonged, accompanied by a smaller aerosol effective radius (R_{eff}) and lower formation/growth rate during heatwaves.

L120-123: During the summer of 2022, a rare heatwave event raged throughout China, especially the Sichuan-Chongqing region of southwest China (Chen et al., 2024; Wang et al., 2024), with the daily maximum temperature exceeding 40 °C lasted for 29 days observed at Beibei meteorological station in Chongqing (Hao et al., 2023).

L142-155: During the observation period, urban Chongqing suffered a rare heatwave (Fig. S1; Chen et al., 2024; Wang et al., 2024), which significantly affected the local transportation and industrial activities (Hao et al., 2023). China Meteorological Administration (CMA) defines heatwaves as three or more consecutive days with daily maximum temperature (T_{max}) above 35 °C

(http://www.cmastd.cn/standardView.jspx?id=2103; Guo et al., 2016; Sun et al., 2014; Tan et al., 2007). Since no unified definition of heatwaves worldwide, the whole study period was categorized into two stages according to CMA's criteria of the daily T_{max} records and the Excess Heat Factor (EHF) metric proposed by Nairn and Fawcett (2014) (Fig. S2a): (1) the normally hot period from 29 July to 6 August (marked as P1); (2) the heatwave-dominated period from August 7-19 (marked as P2) characterized with the consistently occurrence of T_{max} exceeding 38 °C (approximately the last 25^{th} percentile of temperature records for the whole observation period; Fig. S2b).

L313-315: Additionally, the mean CS of the NPF_P events was above 0.015 S⁻¹ (Table S2), which could be considered as the "polluted" NPF day (Shang et al., 2023).

L353-354: The NPF events under heatwaves usually initiated earlier (Fig. S8),

L648-649: In comparison to the P1 NPF_P events, NPF_{C, HW} occurred approximately one hour earlier and the subsequent growth was longer during P2,

Updates in the reference list:

Chen, T., Wang, T., Xue, L., and Brasseur, G.: Heatwave exacerbates air pollution in China through intertwined climate-energy-environment interactions, Sci. Bull., 69, 2765–2775, https://doi.org/10.1016/j.scib.2024.05.018, 2024.

Nairn, J. R. and Fawcett, R. J. B.: The excess heat factor: A metric for heatwave intensity and its use in classifying heatwave severity, Int. J. Environ. Res. Public Health, 12, 227–253, https://doi.org/10.3390/ijerph120100227, 2014.

Sun, X., Sun, Q., Zhou, X., Li, X., Yang, M., Yu, A., and Geng, F.: Heat wave impact on mortality in Pudong New Area, China in 2013, Sci. Total Environ., 493, 789–794, https://doi.org/10.1016/j.scitotenv.2014.06.042, 2014.

Tan, J., Zheng, Y., Song, G., Kalkstein, L. S., Kalkstein, A. J., and Tang, X.: Heat wave impacts on mortality in Shanghai, 1998 and 2003, Int. J. Biometeorol., 51, 193–200, https://doi.org/10.1007/s00484-006-0058-3, 2007.

Wang, N., Du, Y., Chen, D., Meng, H., Chen, X., Zhou, L., Shi, G., Zhan, Y., Feng, M., Li, W., Chen, M., Li, Z., and Yang, F.: Spatial disparities of ozone pollution in the Sichuan Basin spurred by extreme, hot weather, Atmos. Chem. Phys., 24, 3029–3042, https://doi.org/10.5194/acp-24-3029-2024, 2024.

Updated on the Supplement:

The aforementioned Figure 1R has also been added into the Supplement (i.e., Figure S2):

L42-44: Based on the method proposed by Nairn and Fawcett (2014), the Excess Heat Factor (EHF) metric was accordingly calculated for this study (Figure S2a).

RC2. Please provide statistics of NPF events and non-events for both periods. A total of 23 days is divided into 4 categories and conclusions are drawn from a mere one heatwave event. How confidently can you say heatwave(s) promote NPF (based on your results alone)? How about NPF frequency from previous years during the same time period? I also suggest showing an averaged contour plot of particle number size distributions for all these four categories.

Response: We thank the reviewer for this valuable suggestion. As stated in our response to **RC1**, our study is attempted to stress that atmospheric conditions were significantly impacted under the heatwave weather, further influencing the corresponding NPF and aerosol physicochemical properties. We have followed the suggestion and provided the frequency results of NPF days, non-event days and undefined days during both periods in Figure S4a, and the averaged contour plots of PNSD, as well as D_{mode}, R_{eff}, and CS for these four categories were given in Figure S6.

Due to the data availability, we have compared the PNSDs measured at the same site in summer of 2023, which was similarly divided into P1²⁰²³ and P2²⁰²³ periods with the same dates as that of summer 2022. The frequencies of NPF events during P1²⁰²³ (mean T: 30.5 \pm 3.3 °C) and P2²⁰²³ (mean T: 32.9 \pm 3.1 °C) in 2023 were generally identical to that for 2022 (Figure R2), likely suggesting that heatwaves did

not significantly change the occurrence of NPF events. However, the mean star time and growth end time of NPFc, HW events were 9:36 LT (11:07 LT) and 20:37 LT (19:20 LT), respectively, during the P2 period (P2²⁰²³ period) (Figure R4). This signifies that NPF_{C, HW} events occurred earlier and the subsequent growth was prolonged during the P2 heatwave-dominated period. Besides, the impacts of heatwaves on the subsequent growth of NPF events were rather evident. For instance, aerosol Reff was much smaller on the P2 NPFC, HW days. As shown in Figure S6, the Reff and particle D_{mode} nearly kept at a same level below/approaching 50 nm during the subsequent growth on the P2 NPF_{C, HW} days. Differently, the R_{eff} was generally above 50 nm and larger than D_{mode} for both P1 NPF_P cases and non-event days. Moreover, $R_{\rm eff}$ for $P2^{2023}$ NPF days (123.9 \pm 9.5 nm) were significantly higher than those for P2 NPF_{C, HW} days (102.8 \pm 12.4 nm) (Figure R3b2), whereas comparable to that of the P1 NPF_P days (124.8 \pm 10.7 nm). These differences highlight the uniqueness of P2 NPF_{C, HW} events affected by heatwaves despite of insignificant discrepancy in the occurrence frequency of NPF, which merits more in-depth exploration. Further studies on the mechanisms underlying these changes, particularly under extreme weather conditions, are therefore highly recommended.

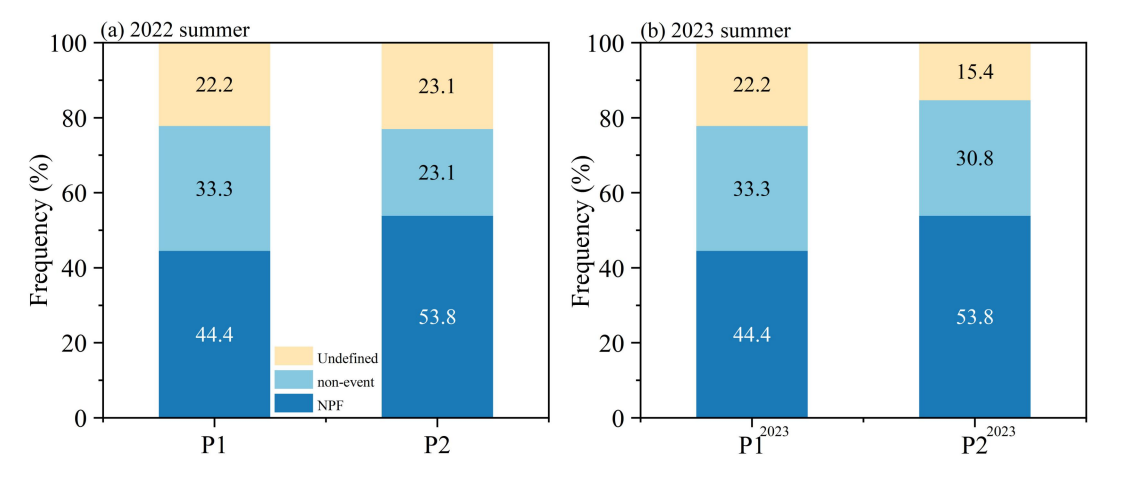


Figure R2. The occurrence frequencies of NPF, non-event and Undefined days during P1 ($P1^{2023}$) and P2 ($P2^{2023}$) periods of summer 2022 (2023).

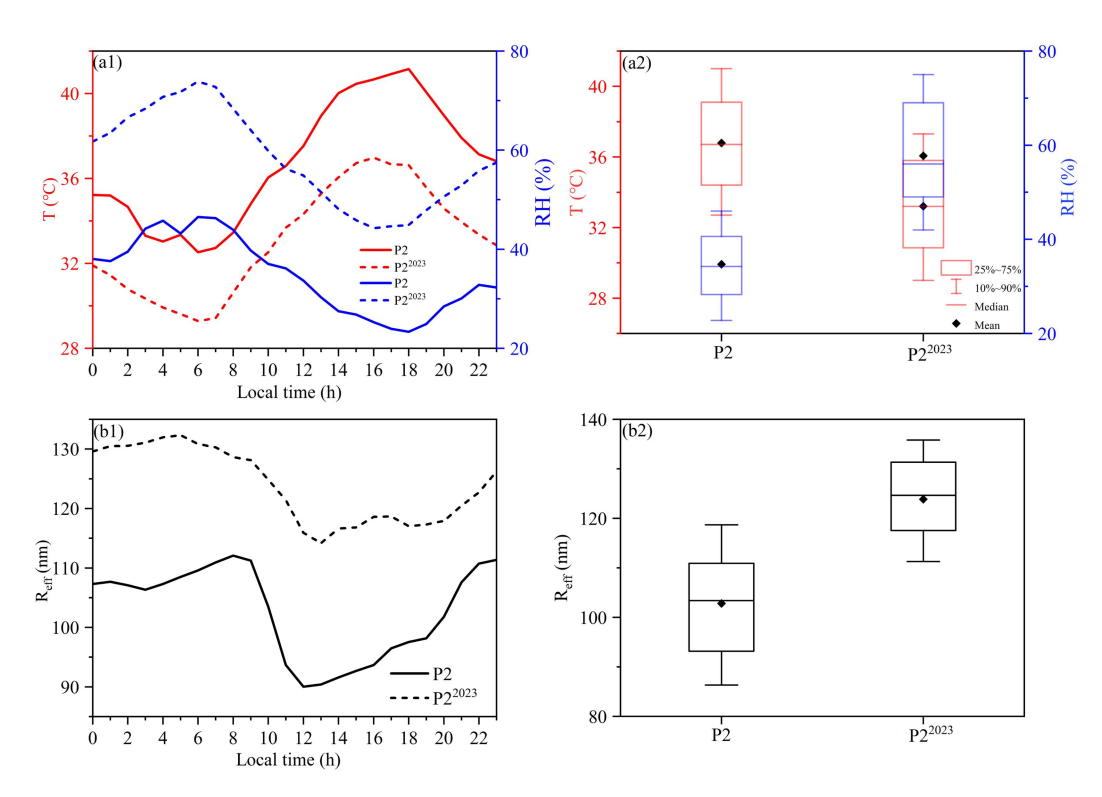


Figure R3. The diurnal variations of T and RH (a1), as well as R_{eff} (b1) on the P2 NPFC, HW and $P2^{2023}$ NPF days, and the corresponding box plots of T, RH (a2) and R_{eff} (b2).

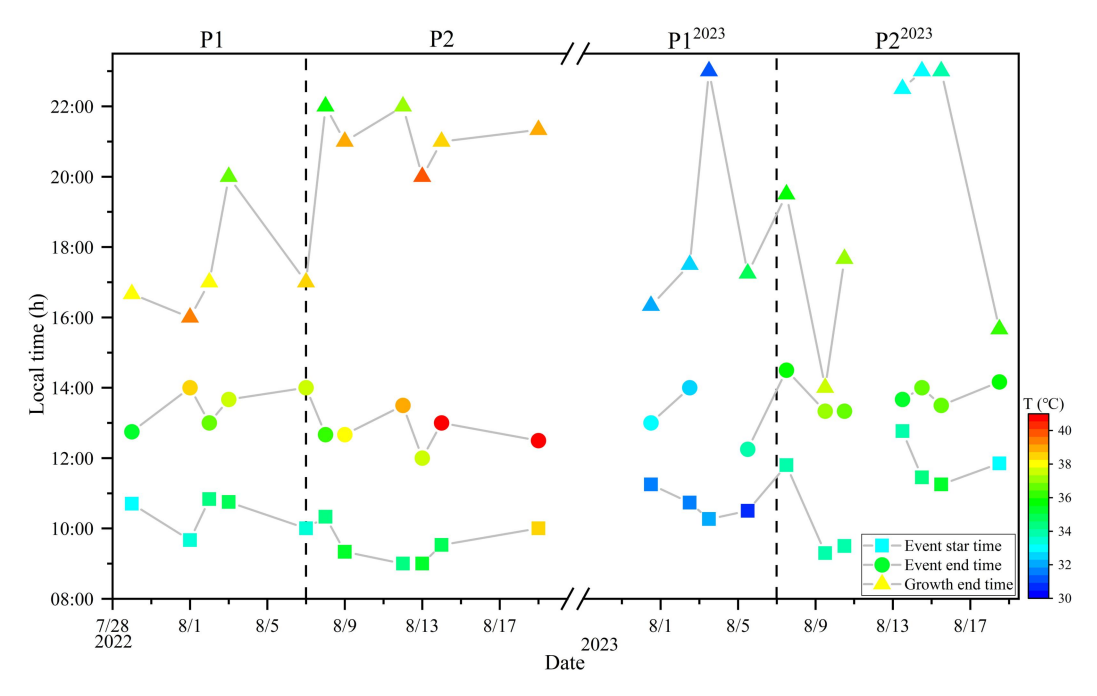


Figure R4. The start and end time of NPF, along with the subsequent growth end time and their corresponding temperature levels during NPF events in summer 2022 and the same period in summer 2023.

Considering the above aspects, we have updated the manuscript as follows:

L271-273: The particle number size distribution data suggested that NPF events appeared in about half the number of observation days (Fig. 1i), with an overall occurrence frequency of 52.4% (Fig. S4a).

L349-350: To further investigate the effect of heatwave on NPF events, the diurnal variations of PNSD, R_{eff} and particle mode diameter (D_{mode}) are shown in Fig. S6.

L353-357: The NPF events under heatwaves usually initiated earlier (Fig. S8), with the number concentration of nucleation mode particles (N_{Nuc}) in P2 NPF_C, HW cases peaked about an hour earlier in comparison to NPF_P days (Fig. S7a). The D_{mode} on P2 NPF_C, HW days also reached its minimum earlier than that on P1 NPF_P days (Fig. S6).

L369-379: In addition, aerosol R_{eff} was significantly smaller on the NPF_{C, HW} days under heatwave conditions. The R_{eff} and D_{mode} nearly kept at a same level below/approaching 50 nm during the subsequent growth on the P2 NPF_{C, HW} days, while the R_{eff} was generally above 50 nm and larger than D_{mode} for both P1 NPF_P cases and non-event days (Fig. S6). The diurnal patterns of aerosol volume concentrations for different size modes were similar to that of aerosol number concentrations during NPF events (Fig. S7b1-b3). However, both the R_{eff} of Aitken mode particles (R_{Ait}) and accumulation mode particles (R_{Acc}) were smaller during P2 NPF_{C, HW} events than that of P1 NPF_P events (Fig. S7c2-c3), which may further influence size-dependent aerosol optical and hygroscopic properties (e.g., $\sigma_{sca, 525}$, HBF, SAE, f(RH)).

Updated on the Supplement:

L131-133: The specific dates for NPF and non-event classifications were summarized in Table S1, and the frequencies of NPF, non-event and Undefined days during both periods were shown in Figure S4a.

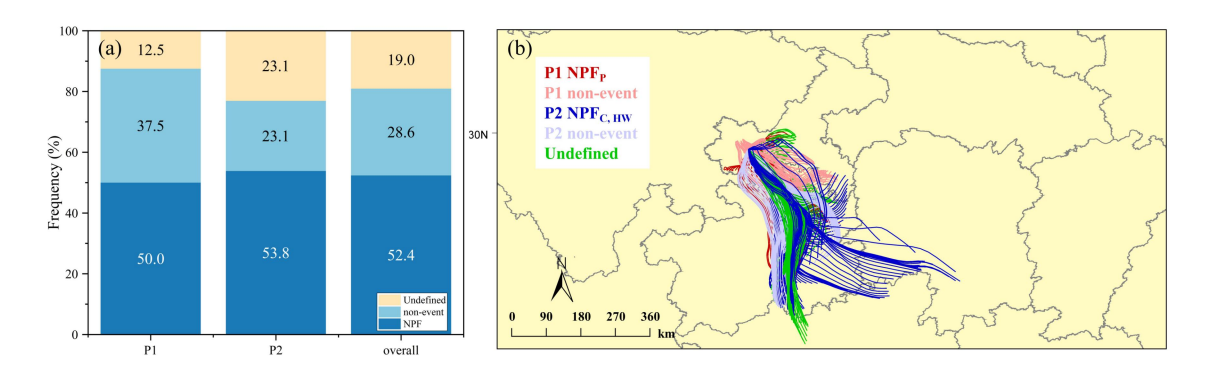


Figure S4. (a) The occurrence frequencies of NPF, non-event and Undefined days during P1, P2 and the whole observation periods. (b) The 48-h air-mass back trajectories during the study period.

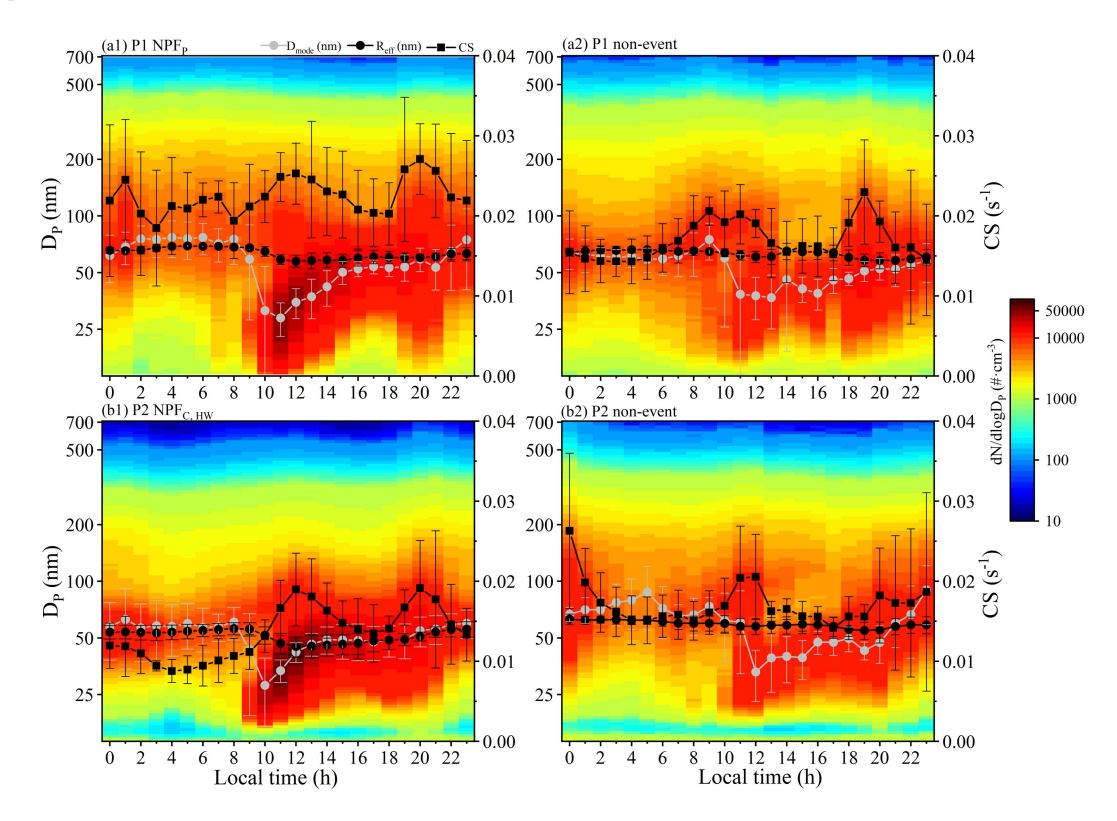


Figure S6. Diurnal variations of PNSDs, D_{mode} , R_{eff} , and CS during P1 and P2 NPF days (a1, b1) and non-event days (a2, b2), the error bars stand for \pm one standard deviations.

RC3. Air mass history plays also a critical role in new particle formation processes. Consider showing an airmass history analysis (source and altitude) using HYSPLIT or Flexpart or similar models. The wind direction during the P2 period appears to be persistently east-southeast.

Response: We agree that air mass history could facilitate the analysis on NPF events. As suggested, the 48-h back trajectories of air mass at 500 m altitude above the site during this study period were calculated using the HYSPLIT (Hybrid Single-Particle Lagrangian Integrated Trajectory) 4 model developed by NOAA (Stein et al., 2015). Results were visualized by MeteoInfoMap (version 3.9.9) (Chen et al., 2021; Tian et al., 2021; Wang, 2014), as shown in the above Figure S4b. The predominant southerly breeze during the summer campaign likely suggests that some other factors could affect the NPF events more significantly in P1 and P2 periods.

We have added the discussion on back trajectories analysis in the revised manuscript.

In the main text:

L205-207: The descriptions of simultaneous meteorological and air quality data can be found in Sect. S4, and the 48-h backward trajectory analysis was given in Sect. S5 of the supplement.

L297-302: The backward trajectory analysis revealed that the southerly breeze was predominant during the study period (Fig. S4b). Although the surface wind vector slightly varied between the P1 and P2 periods, this consistency in air mass origins suggests that some other factors (e.g., changes in environmental conditions and emissions of gaseous precursors under heatwaves) could have played a crucial role in modulating NPF events.

In the Supplement:

L133-137: By using the HYSPLIT (Hybrid Single-Particle Lagrangian Integrated Trajectory) 4 model developed by NOAA (Stein et al., 2015), the 48-h back trajectories of air masses at 500 m altitude above the observation site during this study period were calculated and visualized by MeteoInfoMap (version 3.9.9; Figure S4b) (Chen et al., 2021; Tian et al., 2021; Wang, 2014).

Updates in the reference list of Supplement:

Chen, J., Wu, Z., Chen, J., Reicher, N., Fang, X., Rudich, Y., and Hu, M.: Size-resolved atmospheric ice-nucleating particles during East Asian dust events,

Atmos. Chem. Phys., 21, 3491–3506, https://doi.org/10.5194/acp-21-3491-2021, 2021.

Stein, A. F., Draxler, R. R., Rolph, G. D., Stunder, B. J. B., Cohen, M. D., and Ngan, F.: Noaa's hysplit atmospheric transport and dispersion modeling system, Bull. Am. Meteorol. Soc., 96, 2059–2077, https://doi.org/10.1175/BAMS-D-14-00110.1, 2015.

Tian, J., Guan, H., Zhou, Y., Zheng, N., Xiao, H., Zhao, J., Zhang, Z., and Xiao, H.: Isotopic source analysis of nitrogen-containing aerosol: A study of PM2.5 in Guiyang (SW, China), Sci. Total Environ., 760, 143935, https://doi.org/10.1016/j.scitotenv.2020.143935, 2021.

Wang, Y. Q.: MeteoInfo: GIS software for meteorological data visualization and analysis, Meteorol. Appl., 21, 360–368, https://doi.org/10.1002/met.1345, 2014.

RC4. How is aerosol optical enhancement factor related to particle diameter for both cases (RH<30% and RH=85%)? You may include a figure in the supplementary if you feel relevant.

Response: In our study, the aerosol optical enhancement factor (f(RH)) was determined by measuring the ratio of the total scattering coefficients of the aerosol population under dry (RH <35%) and humidified (RH = 85 \pm 1%) conditions. Specifically, we measured the total scattering coefficient of the aerosol population, which integrated contributions from all the particle sizes rather than specific size bins. As a result, the f(RH) values obtained in this study represent the bulk optical enhancement of the aerosol population, independent of the particle diameter.

RC5. Page 16, Section 3.4: I don't understand why Figure 4 (c & d) focuses on non-events. I suggest showing results in a similar fashion for all four categories in Fig 4c and 4d, and also in Fig 5. Lines 415-418: Are you referring to NPF and

non-events during P2? the subsequent discussion appears to be for non-events during P2? Please update Figure 4 and 5, and revise this section thoroughly.

Response: Following the suggestion, we have merged Fig. S11a1-a2 into Figure 4 and Fig. S11b1-b2 into Figure 5, the original Fig.S11 was removed from the supplement. This revision better demonstrates the relationships between f(RH) and R_{eff} , as well as f(RH) and SAE, among different categories (i.e., both NPF and non-events during P1 and P2 periods).

Yes, the discussion in Lines 415-418 indeed refers to non-event days during P2. We have revised the manuscript to avoid misunderstanding.

L464-466: ...primarily via photochemical reactions and further intensified by heatwaves during the non-event day particularly of the P2 period...

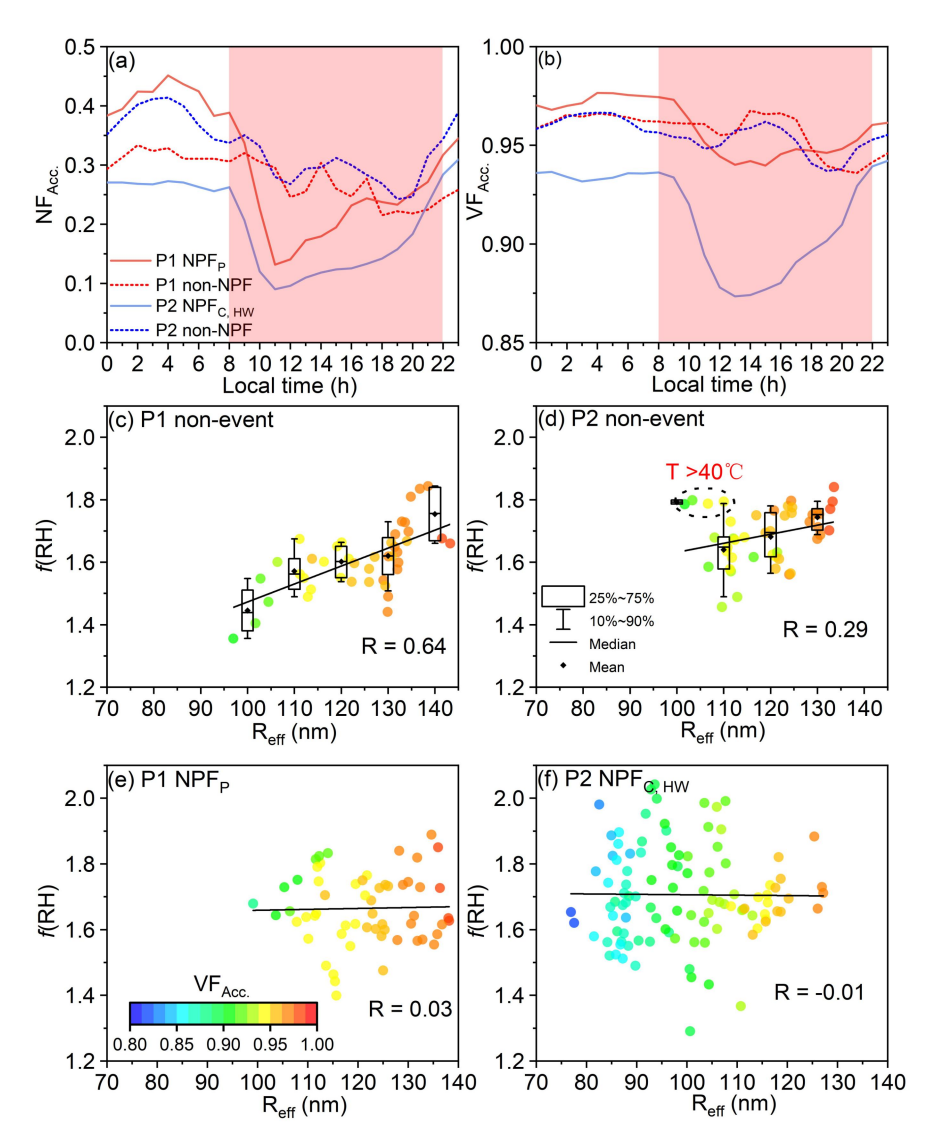


Figure 4. Diurnal variations of **(a)** the number fraction (NF_{Acc.}) and **(b)** volume fraction of accumulation mode particles (VF_{Acc.}) on P1 (red) and P2 (blue) NPF days (solid line), as well as non-event days (dash line). The time window of 08:00-22:00 LT was shaded in red. The relationship of f(RH) with R_{eff} and $VF_{Acc.}$ (as indicated by the colored dots) on P1 **(c)** and P2 non-event days **(d)**, as well as on P1 **(e)** and P2 **(f)** NPF days during the 08:00-22:00 LT time window.

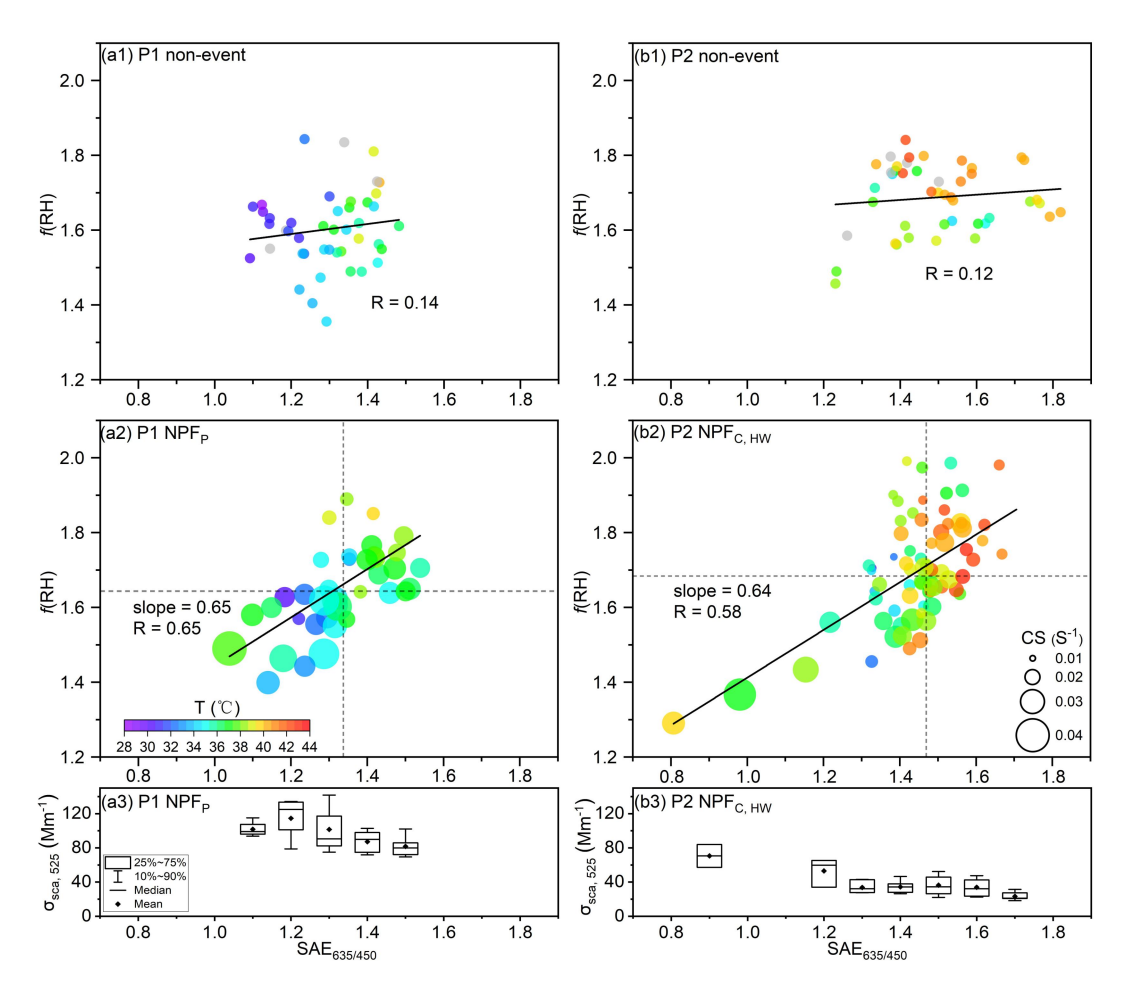


Figure 5. The relationship between f(RH) and $SAE_{635/450}$, as well as temperature (as indicated by the color of dots, missing values are represented in gray) and CS (as denoted by the size of circles), on P1 non-event days (a1), NPF_P days (a2) during the 08:00-22:00 LT time window. The vertical (horizontal) dash line represents the median value of $SAE_{635/450}$ (f(RH)). (a3) The corresponding σ_{sca} , 525 under different $SAE_{635/450}$ levels on P1 NPF_P days. (b1-b3) The same but for P2 period.

RC6. Why GR (<25nm, 25-100 and >100 nm) and FR are not reported and compared between the event types based on SMPS data.?

Response: We have performed additional calculations of FR and GR of different size ranges following the methodologies introduced by Kulmala et al. (2012), and the specific results were summarized in Table R1. The results indicate that both FR and GR (<25 nm) of new particles on the P1 NPF_P days were generally higher than those for P2 NPF_{C, HW} days. Notably, when aerosol particle sizes are in the range of tens of

nanometers, their sources are significantly influenced by primary emissions and transport processes, which may introduce errors into the calculation results (Shang et al., 2023). Furthermore, when aerosol particle sizes exceed 80 nm, the "maximum concentration method" cannot effectively calculate aerosol growth rates (Dal Maso et al., 2005; Kulmala et al., 2012).

Table R1. The FR (Formation Rate) and the GR of different size ranges on the NPF days in this study

Date	FR (cm ⁻³ s ⁻¹)	GR<25 nm (nm·h ⁻¹)	GR _{25-40 nm} (nm·h ⁻¹)	GR _{40-60 nm} (nm·h ⁻¹)	GR _{60-80 nm} (nm·h ⁻¹)
7.29	15.78	9.98	/	/	/
8.1	10.06	14.42	/	1.55	/
8.2	/	/	5.67	5.27	4.81
8.3	25.47	16.63	8.57	13.78	16.65
8.7	6.22	10.08	8.79	/	/
8.8	/	/	15.53	6.38	6.22
8.9	8.47	12.09	9.82	6.21	1.59
8.12	18.98	5.76	5.86	3.91	6.6
8.13	/	/	8.27	4.01	8.3
8.14	/	/	13.37	4.21	2.07
8.19	/	/	2.88	1.72	8.3

We have added the above mean FR and GR results into the original Table S2, and updated the corresponding discussion in the revised manuscript:

In the main text:

Abstract: accompanied by a smaller aerosol effective radius (R_{eff}) and lower formation/growth rate during heatwaves.

L190-193: representative parameters for NPF events, e.g., the formation rate (FR) and growth rate (GR) of new particle, condensation sink (CS) and coagulation sink (CoagS) (Dal Maso et al., 2005; Kulmala et al., 2012). More details are provided in the supplement (Sect. S5).

L364-365: Given that the growth rates of new particles were generally lower during $P2 NPF_{C, HW}$ events (Table S2),

L382-383: (2) lower FR and GR of particles under the cleaner environment (Table S2);

L500-502: One is related to the smaller aerosol R_{eff} (with a larger SAE) due to the lower FR and GR, likely influenced by the evaporation of newly-formed unstable clusters and particle coatings under heatwaves

L646-648: NPF_C, HW events that occurred during the heatwave P2 period were characterized with lower CS, CoagS, FR and GR, as well as smaller R_{eff} and D_{mode} , than P1 NPF_P cases.

In the Supplement:

L126-130: Using the measured PNSD data, NPF events were identified according to the criteria raised by Dal Maso et al. (2005), and the key parameters related to NPF events (e.g., formation rate (FR) and growth rate (GR) of new particles, condensation sink (CS) and coagulation sink (CoagS)) could be derived following the methodologies introduced by Dal Maso et al. (2005) and Kulmala et al. (2012).

Updates in the reference list of Supplement:

Dal Maso, M., Kulmala, M., Riipinen, I., Wagner, R., Hussein, T., Aalto, P. P., and Lehtinen, K. E. J.: Formation and growth of fresh atmospheric aerosols: Eight years of aerosol size distribution data from SMEAR II, Hyytiälä, Finland, Boreal Environ. Res., 10, 323–336, 2005.

Technical comments:

RC7. Abstract: "Heatwaves triggered NPF earlier" – please quantify. You may want to plot sunrise and sunset times in Fig. S5. Define NPF event end time and growth event end time somewhere in the text.

Response: As mentioned in our response to **RC1** (Referee #2), we have revised the corresponding statement in the abstract. Given the insignificant variability in both sunrise and sunset times during the study period (i.e., just within half an hour

discrepancy; Figure R5), we have included such information into the main text instead of adding these data in Figure S5. The definitions of the NPF event end time and growth end time were accordingly updated in the Supplementary.

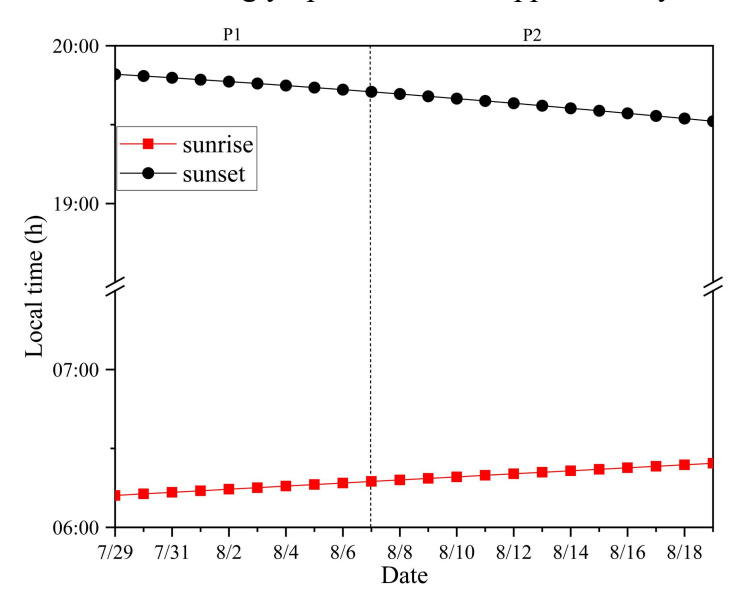


Figure R5. Variations in sunrise and sunset times during the study period.

Updates in the main text:

Abstract: Compared to the NPF_P events, NPF_{C, HW} occurred approximately one hour earlier and the subsequent growth was prolonged, accompanied by a smaller aerosol effective radius (R_{eff}) and lower formation/growth rate during heatwaves.

L357-361: Since the sunrise and sunset time did not significantly vary within the study period (i.e., less than a half hour discrepancy), heatwaves likely provided more favorable conditions (e.g., enhanced volatile gaseous emissions, low RH; Bousiotis et al., 2021; Hamed et al., 2007; Wang et al., 2024) for the occurrence of NPF events in urban Chongqing.

Updates in the Supplement:

L160-169: The specific start and end time of NPF, along with the subsequent growth end time, during NPF events were displayed in Figure S8. The NPF event end time is defined as the moment when the formation of new nucleation-mode particles (diameter <25 nm) ceases, specifically identified by the absence of a notable increase in sub-25 nm particles (Dal Maso et al., 2005; Hamed et al., 2007; Kerminen et al., 2018). The growth event end time refers to the time when the newly formed particles

stop growing, typically due to the depletion of low-volatility vapors or particle coagulation (Dal Maso et al., 2005; Kerminen et al., 2018). This can be observed as the stabilization of particle diameters in the Aitken/accumulation mode, marked by a flattening of the growth trajectory in the PNSD plot (Figure 1i).

Updates in the reference list of the Supplement:

Hamed, A., Joutsensaari, J., Mikkonen, S., Sogacheva, L., Dal Maso, M., Kulmala, M., Cavalli, F., Fuzzi, S., Facchini, M. C., Decesari, S., Mircea, M., Lehtinen, K. E. J., and Laaksonen, A.: Nucleation and growth of new particles in Po Valley, Italy, Atmos. Chem. Phys., 7, 355–376, https://doi.org/10.5194/acp-7-355-2007, 2007.

Kerminen, V. M., Chen, X., Vakkari, V., Petäjä, T., Kulmala, M., and Bianchi, F.: Atmospheric new particle formation and growth: Review of field observations, Environ. Res. Lett., 13, https://doi.org/10.1088/1748-9326/aadf3c, 2018.

RC8. Consider an obvious abbreviation for event classification – relatively polluted period (P1) to be indicated as $NPF_{polluted}$ and clean heatwave-induced to be indicated as $NPF_{clean,\,HW}$

Response: We have accepted this suggestion and updated throughout the manuscript and figures (i.e., NPF_P and NPF_{C, HW}):

L284-287: Correspondingly, NPF events occurring during the relatively polluted P1 period (as detailed in section 3.2) were defined as NPF_P, while cases during the cleaner and heatwave-dominated P2 period were classified as NPF_{C, HW}.

RC9. All figure captions should clearly mention what is being plotted, time resolution, time (local to UTC), etc and they should be self-explanatory.

Response: We have updated all the figures, and all the time in the text was labelled as local time (LT).

RC10. There is an interesting recent paper by Garmash et al., 2024, the authors should consider citing and discussing it – DOI 10.1088/1748-9326/ad10d5

Response: We appreciate the recommendation of this article, which indeed provides support for our study. We have cited this paper and discussed accordingly in the revised manuscript:

L336-341: However, it is reported that excessive heat can increase the evaporation rate of critical acid-base clusters during the nucleation process and reduce the stability of initial molecular clusters (Bousiotis et al., 2021; Kurtén et al., 2007; Zhang et al., 2012), in line with a recent study that NPF events were weaker during heatwaves in Siberian boreal forest due to the unstable clusters (Garmash et al., 2024).

L379-382: The decrease in $R_{Ait.}$ and $R_{Acc.}$ during heatwaves could be attributed to three factors: (1) evaporation of the outer layer of particles and unstable clusters due to heatwaves (Bousiotis et al., 2021; Cusack et al., 2013; Deng et al., 2020; Garmash et al., 2024; Li et al., 2019);

Updates in the reference list:

Garmash, O., Ezhova, E., Arshinov, M., Belan, B., Lampilahti, A., Davydov, D., Räty, M., Aliaga, D., Baalbaki, R., Chan, T., Bianchi, F., Kerminen, V. M., Petäjä, T., and Kulmala, M.: Heatwave reveals potential for enhanced aerosol formation in Siberian boreal forest, Environ. Res. Lett., 19, https://doi.org/10.1088/1748-9326/ad10d5, 2024.

RC11. Particle size distribution measurement size range (and number of bins), and time resolution may be mentioned.

Response: We have updated it accordingly in the Supporting Information, S5:

S5. Particle number size distribution measurements

During the field observation, every 3-min PNSD and particle volume size distribution (PVSD) was measured by a SMPS, which consisted of a soft X-Ray neutralizer (model 3088, TSI Inc.), a differential mobility analyzer (model 3081, TSI Inc.), and a condensation particle counter (model 3775, TSI Inc.) (Dominick et al., 2018; Rissler et al., 2006). The SMPS was operated at a sheath/sample flow rate of

3.0/0.3 LPM, and the detected size range was 14.1-710.5 nm with 110 size bins. Data inversion of measured particle size distributions was achieved with the Aerosol Instrument Manager software (AIM, TSI Inc.), including the multiple charge and diffusion corrections (Denjean et al., 2015; Rosati et al., 2022).

Updates in the reference list of Supplement:

Denjean, C., Formenti, P., Picquet-Varrault, B., Camredon, M., Pangui, E., Zapf, P., Katrib, Y., Giorio, C., Tapparo, A., Temime-Roussel, B., Monod, A., Aumont, B., and Doussin, J. F.: Aging of secondary organic aerosol generated from the ozonolysis of α-pinene: Effects of ozone, light and temperature, Atmos. Chem. Phys., 15, 883–897, https://doi.org/10.5194/acp-15-883-2015, 2015.

Rosati, B., Isokääntä, S., Christiansen, S., Jensen, M. M., Moosakutty, S. P., De Jonge, R. W., Massling, A., Glasius, M., Elm, J., Virtanen, A., and Bilde, M.: Hygroscopicity and CCN potential of DMS-derived aerosol particles, Atmos. Chem. Phys., 22, 13449–13466, https://doi.org/10.5194/acp-22-13449-2022, 2022.

RC12. How was MLH obtained? All data and methods must be explicitly stated.

Response: We have adjusted the descriptions:

S4. Meteorological and air quality data

All the contemporary hourly meteorological datasets including relative humidity (RH), temperature (T), visibility (VIS), wind speed (WS), wind direction (WD), precipitation were obtained from the Integrated Surface Database from the U.S. National Centers for Environmental Information (https://ncdc.noaa.gov/isd) (Wan et al., 2023; Xu et al., 2020), and the mixing layer height (MLH) data were achieved from China Meteorological Administration in this study.

RC13. Page 4, line 127 -130: consider revising. The data/event sample is too small to draw implications for climate.

Response: We appreciate this suggestion and have updated the Introduction as below:

L134-136: This study will further enrich insights into the potential environmental impacts due to variations in the aerosol optical hygroscopicity and size distribution, specifically under weather extremes (e.g., heatwaves) with the changing climate.

RC14. Page 5, Line 147-149: If I understand correctly, the authors deployed two nephelometers, one with a humidification unit and the other without. I would suggest giving explicit details of how the measurements were conducted.

Response: Yes, we deployed two nephelometers in parallel to measure the aerosol scattering coefficients in both dry and wet conditions. We have updated the details to clarify this point:

L161-168: Ambient air was firstly dried through a Nafion dryer (model MD-700, Perma Pure LLC) to ensure RH <35%, then split into two streams for both dry and humidified nephelometers operated in parallel. The flowrate for each nephelometer was 2.6 LPM. The aerosol scattering ($\sigma_{sca, \lambda}$) and backscattering coefficients ($\sigma_{bsca, \lambda}$) were detected in a dry state (RH <35%) and at a controlled RH level of $85 \pm 1\%$, respectively, with the humidification efficiency regulated automatically by a temperature-controlled water bath. More details on the home-built humidified nephelometer system are available in Kuang et al. (2017, 2020) and Xue et al. (2022).

RC15. Page 7, Line 212: chemical analysis results are plotted in Fig. S2, correct it.

Response: Updated.

L194-195: Results of the offline chemical analysis with TSP filter samples are provided in Sect. S3 and Fig. S3.

RC16. Page 7, Line 220: "Fig." S4? I cannot find meteorological and air quality data. Or do you mean Fig.2? Please check all figures numbering and citations in the text.

Response: We have checked and corrected all the figures, texts and tables numbering and citations.

RC17. Page 18, Lines: 443-445, consider revising the sentence starting "In this sense...." What pollution level are you referring to?

Response: We have revised it as below:

L493-496: Given that larger $\sigma_{sca, 525}$ values typically indicate the condition of a higher aerosol loading, f(RH) increased with SAE whereas decreased with $\sigma_{sca, 525}$, or rather the pollution level, during NPF days.

RC18. Page 18, Lines:445, Remove "Meanwhile"

Avoid unnecessary use of "pretty" (page 14, line 351), "relatively", "meanwhile", "In this sense" as above, etc. throughout the manuscript. Also Page 3, line 97 "there have been a great many studies" – looks unnecessary and no study is cited either. Simply say "Previous studies showed...." and cite relevant studies.

Response: We have accordingly adjusted the corresponding expressions throughout the manuscript.

RC19. How was the aerosol effective radius calculated? Figures S4c1, c2, and c3 are unclear to me. Further, authors should show how the particle mode diameter behaved during P1 and P2 (averaged diurnal variation) for both event types and the condensation sink

Response: The calculation of R_{eff} has been given in S5 in the Supplementary, and the detailed description of aerosol R_{eff} can be found in Hansen and Travi (1974), and Grainger et al. (1995). In brief, R_{eff} is the effective mean radius of the aerosol population that can reflect the influence of aerosol size distribution on the light scattering, which depends on the cross-section of particles per unit volume (Hansen and Travi, 1974). Hence, R_{eff} of the nucleation mode (R_{Nuc.}), Aitken mode (R_{Ait.}), and accumulation mode (R_{Acc.}) particles in Figures S7c1-c3 can be accordingly calculated with the aerosol volume and surface area concentrations of different mode particles.

We have added the diurnal variations of D_{mode} , R_{eff} and CS for both event and non-event days in Figure S6, as included in the previous response to **RC2** (Referee #2).

RC20. There are several linguistic errors or issues with sentence phrasing. As I am not a native English speaker, I prefer not to correct them for the authors. I kindly urge authors to thoroughly proofread the manuscript to ensure clarity before submission. This will greatly enhance the readability and overall impact of the work.

Response: Thanks for the suggestion and we have improved the expression of the manuscript.

Anonymous Referee #3

General comments:

This manuscript focus on the aerosol optical hygroscopicity in Chongqing

during three weeks' field campaign using a combination of a home-built

humidified nephelometer system and a scanning mobility particle sizer (SMPS),

the total suspended particle (TSP) filter sampling and following chemical

analysis, as well as the air pollutants data and meteorological data from available

sources.

The measured aerosol scattering coefficients, aerosol optical hygroscopicity

f(RH), and particle number size distribution are reported. Based on the

temperature and aerosol scattering data, the measurement period from July 19

to August 19, 2022 was divided into P1 period and P2 period

(heatwaves-dominated). The authors discussed the characteristics of NPF events

during P1 and P2 periods, the characteristics of the aerosol optical and

hygroscopic properties during P1 NPF and P2 NPF events, and the effects of

f(RH) on aerosol direct radiative forcing.

Response: Thanks for the comments.

Major comments:

RC1. Section 3.3 Characteristics of the aerosol optical and hygroscopic properties during NPF events

As can be seen from Figure S7, Size-dependent light scattering, backscattering and HBF efficiencies showed the particles with diameter less than 100 nm have insignificant contribution to aerosol scattering. If so, why the authors pay more attention on the aerosol optical and hygroscopic properties during NPF events? What the exact meaning of NPF events here? Since there are 4 and 7 NPF days during P1 and P2 period, it is a little bit hard to investigate the influence of heatwaves on NPF events and subsequent impacts on aerosol optical and hygroscopic properties.

Response: As clarified in our responses to Referee #2, the primary focus of this study is the significant changes observed in both NPF events and aerosol optical and hygroscopic properties against the background of heatwaves. NPF events during the heatwave-dominated P2 period exhibited distinct differences in comparison to normal summer conditions during P1, as well as to the same period in 2023 (refer to our responses to **RC1 and RC2** of Referee #2, Figures R3, R4). These differences are expected to further influence aerosol optical and hygroscopic properties.

We acknowledge that newly formed ultrafine particles have a weak contribution to the aerosol light scattering, yet the subsequent growth into larger sizes combined with atmospheric aging of both pre-existing and newly formed particles could significantly impact aerosol optical hygroscopicity, f(RH). In this study, we consistently observed that the aerosol f(RH) was higher on NPF days compared to non-event days in both periods. Furthermore, heatwaves can intensify photochemical aging processes and prolonged the subsequent growth of new particles on P2 NPF_{C, HW} days, resulting in an even higher f(RH) than that for NPF_P days during P1. This agrees with previous studies that atmospheric conditions which are favorable for the occurrence of NPF can also promote the growth of newly formed particles, thereby enhancing aerosol hygroscopicity (Cheung et al., 2020; Wu et al., 2015, 2116). Additionally, NPF events can increase aerosol extinction coefficients compared to

non-event days and even trigger haze pollution (Kulmala et al., 2021; Shen et al., 2011; Sun et al., 2024; Tang et al., 2021), likely suggesting the potential role of amplified aerosol light extinction ability during NPF events. While generally limited contributions, impacts of the ultrafine-mode particles on aerosol optical hygroscopic properties could become more evident through subsequent particle growth in combination with aging processes of both pre-existing and newly formed particles on NPF days, specifically under heatwave weather. This underlines our motivation for investigating aerosol optical and hygroscopic properties in the context of NPF events under normal and heatwave conditions, which are crucial for understanding the impacts of extreme weather events (e.g., heatwaves) on aerosol physicochemical properties with the changing climate.

We have adjusted the title of Section 3.3 into "Characteristics of the aerosol optical and hygroscopic properties on different types of NPF days" and revised the corresponding expression throughout the manuscript, to avoid the misunderstanding that NPF events affect the aerosol optical hygroscopicity predominantly.

RC2. Section 3.5 f(RH)-induced changes in aerosol direct radiative forcing The effect of aerosol hygroscopicity on aerosol direct radiative forcing depends on f(RH) and the ratio of HBF525, RH to HBF525 ratio which were measured in this study. The authors stated the mean HBF_{525, RH} was generally larger than HBF₅₂₅ with the ratios centered around 1.8 and even approached 2.5 on P2 NPF event days (Fig. 6c, Table S2). This result is in contrast with previous results such as from Titos et al. 2021, Xia et al 2023 and so on. The study by Titos et al., 2021 showed the $f_b(RH=85\%)$ were lower than f(RH=85%) based on the data from 22 different sites covering a wide range of site types (Arctic, marine, rural, mountain, urban, and desert). The study of Xia et al 2023 showed the backscatter hygroscopic growth factor was lower than scattering hygroscopic growth factor (Figure 3) based on 2-year measurement in Beijing. This ratio is critical for this conclusion of this section. The authors need to explain why the ratio is so different? Please give more information about the humidified nephelometer operation information such as the time series of the temperature and relative humidity variation inside the nephelometer, the background variation etc.

Response: We appreciate the reviewer's critical comments regarding the discrepancy observed in the ratio of HBF_{525, RH}/HBF₅₂₅ with previous studies. As shown in Figure R6, RH inside the dry (marked as "D") and wet ("W") nephelometers generally maintained stable throughout the study period, with a synchronized fluctuation in the corresponding temperature records. This confirms the stability of the humidified nephelometer system and the reliability of our measurements, thus instrumental artifacts as a cause of the observed "abnormal" HBF ratio could be excluded.

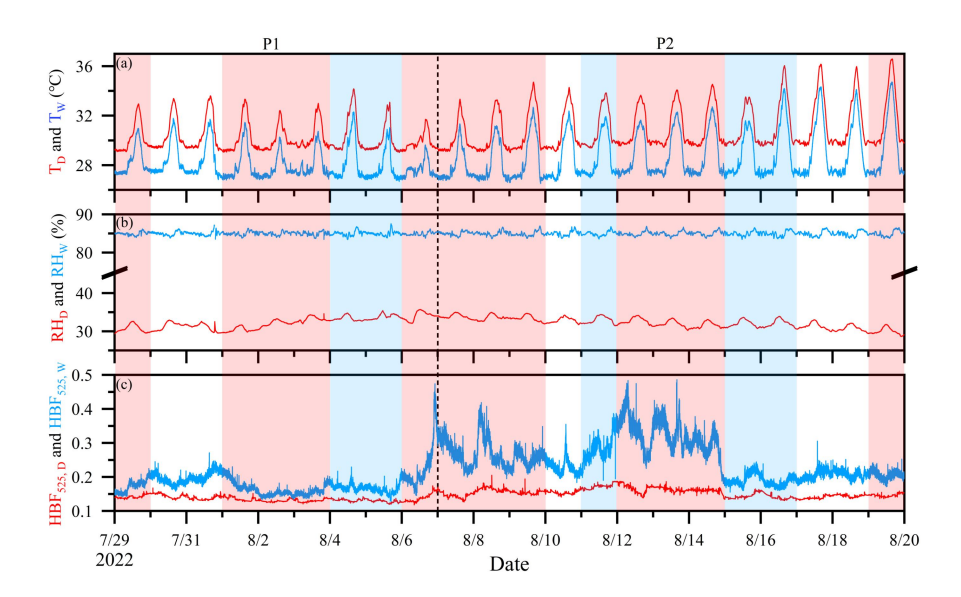


Figure R6. Time series of the (a) temperature, (b) RH inside the "dry" and "wet" nephelometers, and the (c) measured HBF₅₂₅, $_D$ and HBF₅₂₅, $_W$ during the study period. The NPF days and non-event days were shaded in red and blue, respectively.

Our data revealed that the $f_b(RH)$ (aerosol backscattering enhancement factor) exceeded the corresponding f(RH) (Figure R7), suggesting that the increase in $\sigma_{bsca, 525}$ is more pronounced than that of $\sigma_{sca, 525}$ upon hydration. This phenomenon was particularly noticeable on P2 NPF_{C, HW} days, when HBF_{525, RH} significantly higher than HBF₅₂₅ (Figure R6c). Additionally, we derived the asymmetry parameter g (g_{RH}), which positively correlates with the aerosol forward scattering (Andrews et al., 2006; Marshall et al., 1995), from the measured HBF₅₂₅ (HBF_{525, RH}) with the Mie model (Andrews et al., 2006). The g_{RH} were generally smaller than g for the four categories (Figure R7c), implying that the forward (backward) light scattering decreased (increased) after water uptake. This is especially evident on P2 NPF_{C, HW} days, with a much lower level of g_{RH} was observed.

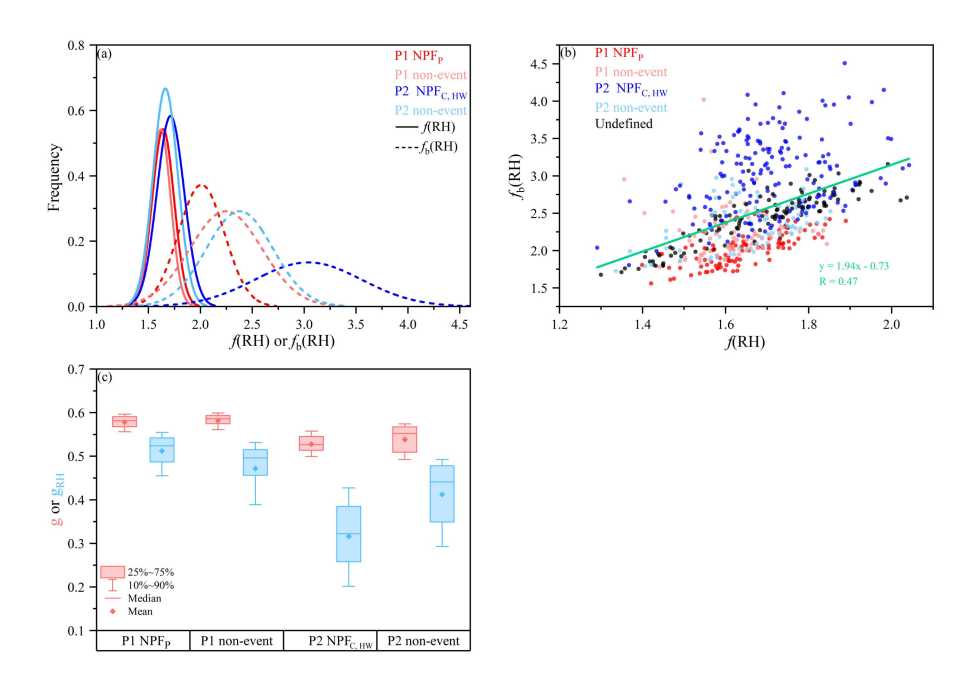


Figure R7. (a) The frequency of f(RH) and $f_b(RH)$ on the NPF days and non-event days during different periods, (b) The relationship between f(RH) and $f_b(RH)$ in this study, (c) The box plots of the HBF₅₂₅ (HBF_{525, RH}) derived $g(g_{RH})$.

There are two potential reasons for these "unique" phenomena. Firstly, the abundant nucleation mode particles could not significantly contribute to aerosol $\sigma_{sca, 525}$ and $\sigma_{bsca, 525}$ during NPF events, even falling below the detection limit of the nephelometer (i.e., 0.3 Mm⁻¹). However, the contributions of these particles to $\sigma_{sca, 525}$ and especially to $\sigma_{bsca, 525}$ were amplified upon humidification in the "wet" nephelometer. As shown in Figure S10a (the original Figure S7), even if these hydrated particles remain small (e.g., below 100 nm), their HBF was significantly higher than that of larger ones and consequently elevated the HBF_{525, RH} levels. This is in line with the simultaneous evolution of aerosol size distributions, which suggest that both R_{eff} and D_{mode} of nucleation-mode particles were almost below/approaching 50 nm on the P2 NPF_{C,HW} days (Figure S6; refer to the response to **RC2** of Referee#2). Secondly, we hypothesize that particle morphology plays a key role in this study. Previous studies have found that backward scattering intensity of non-spherical particles is suggested to be larger (Mishchenko 2009; Yang et al., 2007). Refer to the response to RC10 (Referee #2), particles may be partly evaporated under heatwaves. Additionally, the organic-rich particles might remain non-spherical due to the

efficient evaporation of organic coatings under high temperature conditions (Li et al., 2019), further enhancing the $\sigma_{bsca, 525}$ after hygroscopic growth.

Given the aforementioned possible reasons and our responses to RC1 and RC2 of Referee #2, the unique phenomena of higher $f_b(RH)$ observed during the P2 NPF_{C, HW} days are more pronounced. We acknowledge that these mechanisms merit further validation through molecular-level studies. Future research to investigate the changes in particle morphology, aerosol optical and hygroscopic properties under similar extremely high-temperature conditions (e.g., T >38 °C) is therefore highly recommended.

We have updated the manuscript as follows, and the Figure R7c has been added in the Figure S10 (the original Figure S7):

L574-588: Given that the backward scattering intensity of non-spherical particles is suggested to be much larger than its spherical counterparts at scattering angles between 90° and 150° (Mishchenko 2009; Yang et al., 2007) and that the HBF-derived asymmetry parameter (g) normally correlates positively with the aerosol forward scattering (Andrews et al., 2006; Marshall et al., 1995), the generally smaller g_{RH} results (in comparison to g) confirmed the decrease (increase) in the forward (backward) light scattering after water uptake (Fig. S10b), likely implying the change in the morphological structure of particles. This is particularly evident for P2 NPFC, HW days, with a much lower level of g_{RH} was observed (Fig. S10b). Another possible reason is that although the abundant newly formed particles were generally optically-insensitive, their contributions to σ_{SCa} , 525 and especially to σ_{bSCa} , 525 could be amplified upon humidification. Namely, even if these hydrated particles remained small (e.g., below 100 nm), their HBF was significantly higher than that of larger particles (Fig. S10a), thereby elevating the corresponding HBF525, RH levels during NPF events.

Updates in the reference list:

Andrews, E., Sheridan, P. J., Fiebig, M., McComiskey, A., Ogren, J. A., Arnott, P., Covert, D., Elleman, R., Gasparini, R., Collins, D., Jonsson, H., Schmid, B., and

Wang, J.: Comparison of methods for deriving aerosol asymmetry parameter, J. Geophys. Res. Atmos., 111, 1–16, https://doi.org/10.1029/2004JD005734, 2006.

Marshall, S. F., Covert, D. S., and Charlson, R. J.: Relationship between asymmetry parameter and hemispheric backscatter ratio: implications for climate forcing by aerosols, Appl. Opt., 34, 5–6, 1995.

Comments in details:

RC3. The authors divided the NPF into two classes, one is relatively polluted period and clean cases during heatwave-dominated period

Some sentences are really hard to follow. Such as "Heatwaves triggered NPF earlier and prolonged the subsequent growth." NPF events usually occurred in clean environment with low RH and high sunshine. What evidence does support NPF is triggered by heatwave?

Response: This can refer to our responses to RC1 and RC2 of Referee #2. The NPF events indeed started earlier and the duration of subsequent growth was longer during the heatwave-dominated P2 period, especially compared to the NPF events occurred during the P1 period and the same period in the summer of 2023 (Figure R4). Given that the formation mechanisms of different NPF events are out of the scope of this study, we have revised the corresponding expressions to highlight the differences in both NPF events and aerosol physicochemical properties under heatwave conditions.

RC4. Line 34-36 This sentence is not supported by the data in Table S2 where the f(RH) is almost the same for NPF events and non-event days.

Response: We thank the reviewer for pointing out this issue. The f(RH) values in the original Table S2 were rounded to one decimal place, which made the differences between event and non-event days negligible (but that is not the case, as shown in the below Figure R8). To better reflect the variations in aerosol optical and hygroscopic properties on NPF days and non-event days during different periods, we have revised Table S2 to include f(RH) and other relevant parameters with an additional decimal

place.

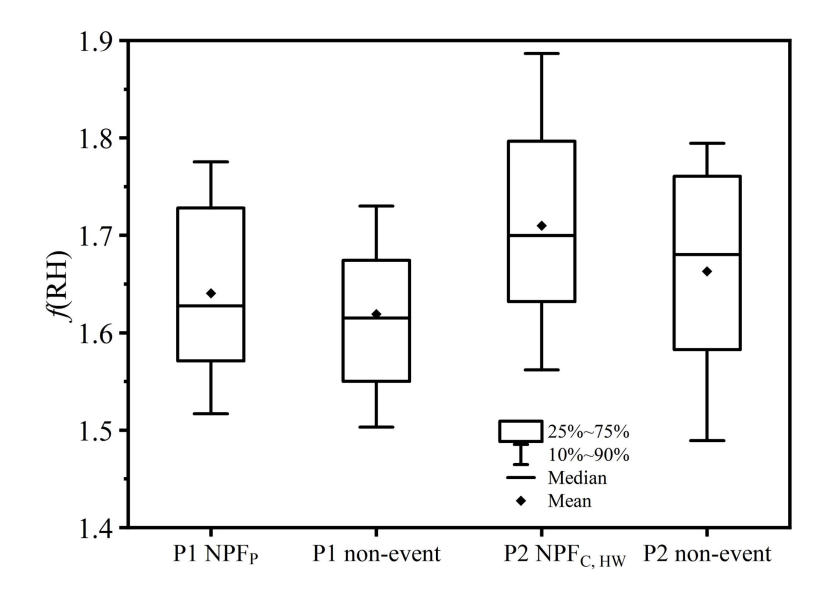


Figure R8. The box plots of f(RH) during P1 and P2 NPF days and non-event days

RC5. Line 90-93 NPF could alter the size distribution thereby aerosol optical properties, nonetheless, there is currently limited research on the impact of NPF on aerosol optical hygroscopicity (Ma et al., 2016; Ren et al., 2021). Since the particles with diameter less than 100nm have insignificant contribution to aerosol scattering just like showed in Figure S7.

Response: The influence of newly formed particles on the aerosol optical properties is insignificant according to the Mie theory, but previous studies have found that the subsequent growth of these new particles can enhance the hygroscopicity and extinction coefficient of aerosol populations (Cheung et al., 2020; Shen et al., 2011; Sun et al., 2024; Wu et al., 2015, 2116). We have revised the manuscript as follows:

L89-98: Numerous studies have demonstrated that f(RH) is influenced by the size distribution, in addition to particle chemical composition (Chen et al., 2014; Kuang et al., 2017; Petters and Kreidenweis, 2007; Quinn et al., 2005). There is currently limited research on the variations in aerosol optical hygroscopicity during NPF days despite significant changes in aerosol size distributions and chemical compositions, partly due to that newly formed particles insignificantly affect the optical properties of aerosols (Kuang et al., 2018). However, previous studies have observed the

enhancement in aerosol hygroscopicity (Cheung et al., 2020; Wu et al., 2015, 2016) and extinction coefficients (Shen et al., 2011; Sun et al., 2024) during the subsequent growth of NPF.

Updates in the reference list:

Shen, X. J., Sun, J. Y., Zhang, Y. M., Wehner, B., Nowak, A., Tuch, T., Zhang, X. C., Wang, T. T., Zhou, H. G., Zhang, X. L., Dong, F., Birmili, W., and Wiedensohler, A.: First long-term study of particle number size distributions and new particle formation events of regional aerosol in the North China Plain, Atmos. Chem. Phys., 11, 1565–1580, https://doi.org/10.5194/acp-11-1565-2011, 2011.

RC6. Line 142-144 As can be seen from Figure 1, the hourly temperature during P2 period (August 7-19) are not always above 40°C which in not consistent with these sentence. In addition, why do you choose the hourly total scattering coefficient at 525 nm of 100 Mm⁻¹ as criteria?

Response: We thank the reviewer for pointing out these contradictions. As explained in our response to **RC1** of Referee #2, the standard for "heatwave-dominated" P2 period was updated accordingly in the main text (Figure R1). We chose 100 Mm⁻¹ (i.e., the last 10^{th} percentile level of all the measured $\sigma_{sca, 525}$ records; Figure R1c) as the criteria for the relatively polluted condition of P1, and none of the hourly $\sigma_{sca, 525}$ during the P2 period (i.e., within 16.1-94.4 Mm⁻¹) exceeded this threshold.

We have revised the corresponding sentence:

L281-284: It should be noted that the hourly $\sigma_{sca, 525}$ values during the P2 period were exclusively below 100 Mm⁻¹ (approximately the last 10^{th} percentile of $\sigma_{sca, 525}$ data, regarded as the threshold value of relatively polluted cases; Fig. S2c), suggesting a much cleaner environment compared to the relatively polluted P1 period.

RC7. Line 171-173 What kind of assumption are behind this calculation of ALWC? What kind of data are used to estimate dry aerosol volume concentration (V_{dry}) by a machine learning method?

Response: In this study, the method for calculating ALWC based on the measurements of humidified nephelometer system was proposed by Kuang et al. (2018). The method mainly consists of two steps, as shown in the flowchart in Figure R9 (redrawn from Figure 8 in Kuang et al., 2018).

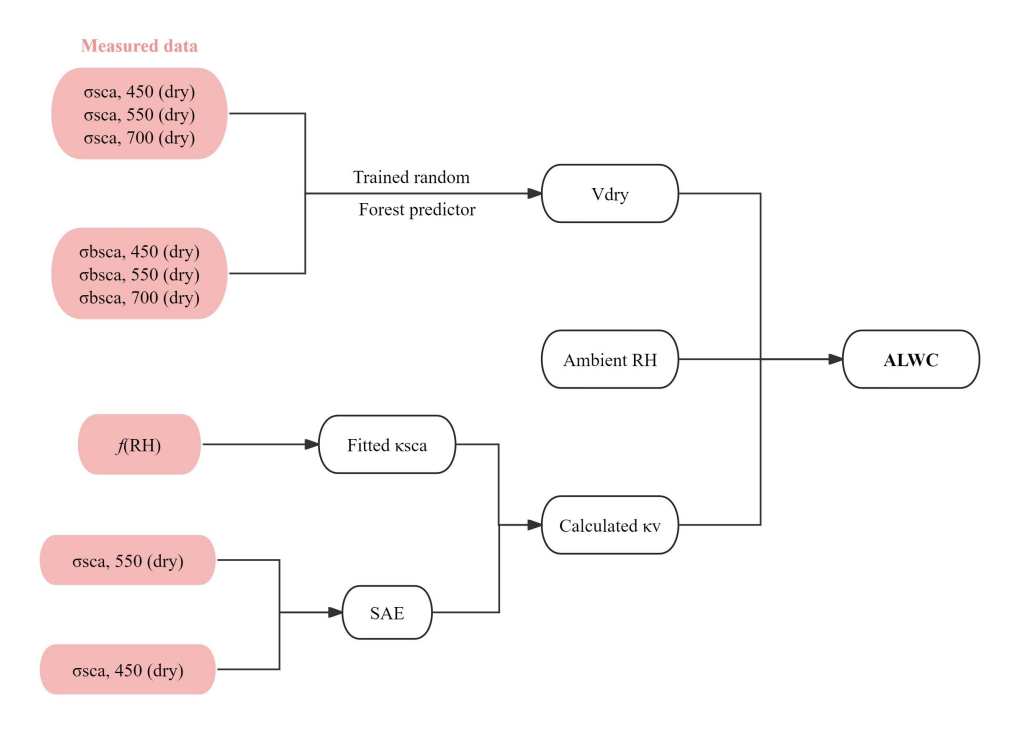


Figure R9. The flowchart of calculating ALWC based on measurements of a three-wavelength humidified nephelometer system (Kuang et al., 2018).

First is the estimation of the dry aerosol volume concentration (V_{dry}). According to the Mie theory, the aerosol $\sigma_{sca, \lambda}$ is roughly proportional to V_{dry} (Pinnick et al., 1980). However, variations of the $\sigma_{sca, \lambda}/V_{dry}$ ratio are largely influenced by PNSD, assuming that other factors affecting aerosol scattering efficiency (e.g., the refractive index and the BC mixing state) vary insignificantly. To derive a simple function describing the relationship between the measured $\sigma_{sca, \lambda}$ and V_{dry} , a machine learning approach is utilized. The random forest model was trained and validated by using datasets of measured optical parameters including the dry $\sigma_{sca, \lambda}$ and $\sigma_{bsca, \lambda}$ at three wavelengths, which can reflect the variations in aerosol size distribution (e.g., the calculated HBF and SAE) (Kuang et al., 2018).

Secondly is the relationship between aerosol f(RH) and volume hygroscopic growth factor ($f_V(RH)$). Based on the κ -Köhler theory (Petters and Kreidenweis, 2007), f(RH) can be parameterized by the aerosol optical hygroscopic parameter κ_{sca} (Brock et al., 2016). Assuming that the Kelvin effect on particles above 100 nm is negligible and that a constant hygroscopic parameter, κ , represents the overall hygroscopicity (Brock et al., 2016), $f_V(RH)$ can be parameterized by the volume hygroscopic parameter, κ_V (Brock et al., 2016; Kuang et al., 2018). Therefore, κ_V is crucial for evaluating the wet volume of aerosols upon hygroscopic growth. Similarly, the variations of the ratio κ_V/κ_{sca} is largely influenced by PNSD (Kuang et al., 2018). Given that SAE can reflect the evolution of PNSD (Kuang et al., 2017, 2018) and assuming κ_{sca} reflects the overall hygroscopicity of aerosols, a lookup table reflecting κ_V/κ_{sca} can be constructed by inputting the measured SAE and κ_{sca} (Kuang et al., 2018). Consequently, $f_V(RH)$ and the corresponding ALWC can be further evaluated.

We have added more details in the Supplement.

L59-62: where the dry aerosol volume concentration (V_{dry}) was estimated with the dry scattering coefficient at three wavelengths utilizing a machine learning method (Kuang et al., 2018).

RC8. The authors mentioned the Nafion dryer are used to dry the ambient air in S1 section in the supplement, what's the total flow for online measurements? Both humidified nephelometers and SMPS share the same $PM_{2.5}$ impactor? More information of SMPS should be given, such as the sheath flow and aerosol

flow, the sheath flow control mode, data retrieval, etc. In supplement S5, is the neutralizer model right?

Response: We have updated the details of the filed observation. We appreciate the reviewer's reminder, and the model of the soft X-ray neutralizer has been corrected (model 3088, TSI Inc.).

In the main text:

L161-164: Ambient air was firstly dried through a Nafion dryer (model MD-700, Perma Pure LLC) to ensure RH <35%, then split into two streams for both dry and

humidified nephelometers operated in parallel. The flowrate for each nephelometer was 2.6 LPM.

In the Supplement:

L36-39: The ambient air was sampled at a flowrate of 16.7 LPM through a $PM_{2.5}$ impactor (model 2000-30EH, URG Inc.) and dried with a Nafion dryer (model MD-700, Perma Pure LLC), to achieve a low relative humidity level (RH <35%) prior to the online aerosol size distribution, optical and hygroscopic measurements.

S5. Particle number size distribution measurements

During the field observation, every 3-min PNSD and particle volume size distribution (PVSD) was measured by a SMPS, which consisted of a soft X-Ray neutralizer (model 3088, TSI Inc.), a differential mobility analyzer (model 3081, TSI Inc.), and a condensation particle counter (model 3775, TSI Inc.) (Dominick et al., 2018; Rissler et al., 2006). The SMPS was operated at a sheath/sample flow rate of 3.0/0.3 LPM, and the detected size range was 14.1-710.5 nm with 110 size bins. Data inversion of measured particle size distributions was achieved with the Aerosol Instrument Manager software (AIM, TSI Inc.), including the multiple charge and diffusion corrections (Denjean et al., 2015; Rosati et al., 2022).

Updates in the reference list of Supplement:

Denjean, C., Formenti, P., Picquet-Varrault, B., Camredon, M., Pangui, E., Zapf, P., Katrib, Y., Giorio, C., Tapparo, A., Temime-Roussel, B., Monod, A., Aumont, B., and Doussin, J. F.: Aging of secondary organic aerosol generated from the ozonolysis of α-pinene: Effects of ozone, light and temperature, Atmos. Chem. Phys., 15, 883–897, https://doi.org/10.5194/acp-15-883-2015, 2015.

Rosati, B., Isokääntä, S., Christiansen, S., Jensen, M. M., Moosakutty, S. P., De Jonge, R. W., Massling, A., Glasius, M., Elm, J., Virtanen, A., and Bilde, M.: Hygroscopicity and CCN potential of DMS-derived aerosol particles, Atmos. Chem. Phys., 22, 13449–13466, https://doi.org/10.5194/acp-22-13449-2022, 2022.

RC9. Line213-215 This sentence is not supported by the Figure S2, where the sum of the measured chemical composition mass concentration is higher than PM_{2.5} mass concentration. It is really hard to understand to use TSP results for the characterization of NPF.

Response: We agree on the concerns about the TSP chemical results used in this study, and we would like to clarify the rationale for their application despite potential limitations.

Previous studies on size-resolved aerosol chemical characterization have suggested that key components (e.g., sulfate, nitrate, and ammonium (SNA in short), OC, EC) of PM_{2.5} (or PM₁₀) were predominantly concentrated in the submicron range (An et al., 2024; Bae et al., 2019; Chen et al., 2019; Duan et al., 2024; Kim et al., 2020; Xu et al., 2024). Specifically, SNA are the predominant fine-mode components (An et al., 2024; Bae et al., 2019; Chen et al., 2019; Kim et al., 2020; Xu et al., 2021, 2024), while organic compounds (OM) could exhibit a broader size distribution due to their diverse sources. For instance, primary organic aerosols (POA) are mainly concentrated in the accumulation mode, while secondary organic aerosols (SOA) may possess a relatively broader size distribution (Duan et al., 2024; Kim et al., 2020; Xu et al., 2021), depending on specific activities and emission sources (e.g., from boilers and kilns during industrial processes) (An et al., 2024). Nevertheless, such emissions with larger particle sizes were relatively limited at our mixed residential-commercial urban site (Chen et al., 2024). The discrepancy in the total mass concentration between the 24-h TSP samples and daily mean PM_{2.5} (of similar temporal variations; original Fig.S2) could be partly attributed to certain secondary organics and crustal elements (e.g., Ca²⁺, Mg²⁺); besides, the boxplot of hourly PM_{2.5} data actually spanned a wider range, which can generally cover the corresponding mass abundance of TSP samples despite some biases (Figure R10).

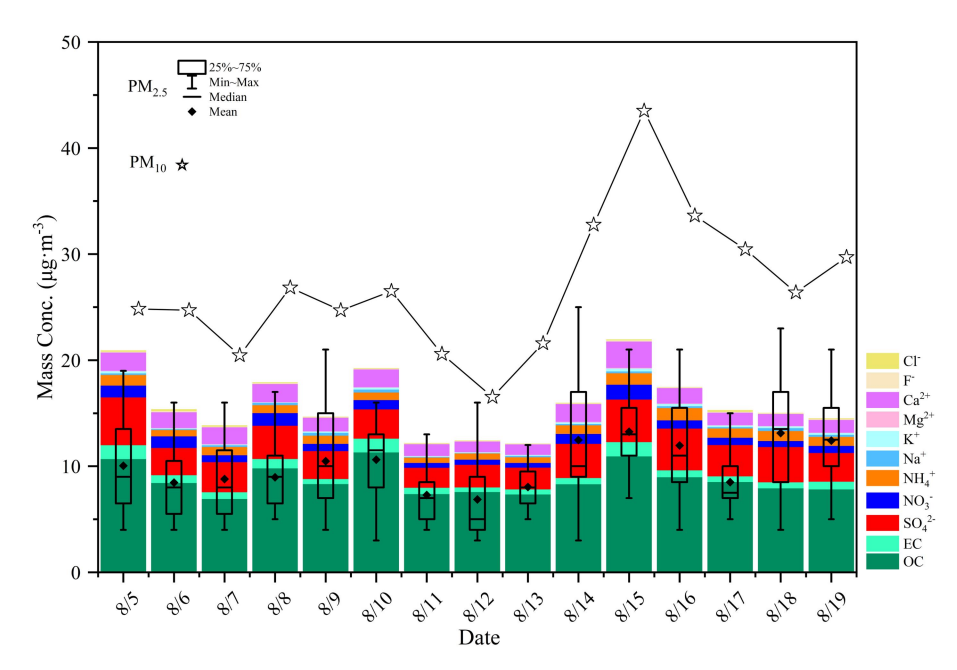


Figure R10. Mass concentrations of the measured chemical components for TSP filter samples, as well as the corresponding daily mean $PM_{2.5}$ and PM_{10} results.

Given the lack of online aerosol chemical characterization on fine particles (e.g., PM_{2.5} or PM₁) and that only the simultaneously collected TSP filter samples were available for offline chemical analysis (e.g., OC, EC, and water-soluble inorganic species), the obtained chemical composition results were utilized mainly for the investigation of aerosol/PM_{2.5} optical and hygroscopic properties in this study (since the mechanisms of different NPF events are out of the scope, as stated in our response to RC3 of Referee #3). The SOC/TOC ratio results derived from the TSP chemical composition data were mainly aimed to assess secondary formation ability and related impacts on aerosol optical and hygroscopic properties, rather than to explore the detailed mechanisms of NPF events. While the use of TSP samples contains some uncertainties, the bulk chemical information remains reasonable for our research objectives (i.e., the optical hygroscopic properties of PM_{2.5}). Future studies of molecular-scale chemical characterization are needed to refine the analysis and deepen understanding on the role of chemical composition in both NPF events and aerosol physicochemical properties.

We have clarified the above points in the revised manuscript and updated accordingly on related figures as below:

L194-205: Results of the offline chemical analysis with TSP filter samples are provided in Sect. S3 and Fig. S3. It should be noted that certain secondary organics and crustal elements (e.g., Ca^{2+} , Mg^{2+}) that could exhibit a broader size distribution may contribute to the observed discrepancy in the total mass concentration between the 24-h TSP samples and daily mean $PM_{2.5}$ (of similar temporal variations; Fig.S3) (Duan et al., 2024; Kim et al., 2020; Xu et al., 2021). Nonetheless, previous studies reported that key components such as SNA (i.e., SO_4^{2-} , NO_3^{-} , and NH_4^{+}) and primary organics of $PM_{2.5}$ (or PM_{10}) were predominantly concentrated within the submicron size range (An et al., 2024; Bae et al., 2019; Chen et al., 2019; Duan et al., 2024; Kim et al., 2020; Xu et al., 2024). While the use of TSP samples contains some uncertainties, the bulk chemical information remains reasonable for characterizing the optical and hygroscopic properties of $PM_{2.5}$.

Updates in the reference list:

Bae, M. S., Lee, T., Schauer, J. J., Park, G., Son, Y. B., Kim, K. H., Cho, S. S., Park, S. S., Park, K., and Shon, Z. H.: Chemical Characteristics of Size-Resolved Aerosols in Coastal Areas during KORUS-AQ Campaign; Comparison of Ion Neutralization Model, Asia-Pacific J. Atmos. Sci., 55, 387–399, https://doi.org/10.1007/s13143-018-00099-1, 2019.

Chen, Q., Mu, Z., Song, W., Wang, Y., Yang, Z., Zhang, L., and Zhang, Y. L.: Size-Resolved Characterization of the Chromophores in Atmospheric Particulate Matter From a Typical Coal-Burning City in China, J. Geophys. Res. Atmos., 124, 10546–10563, https://doi.org/10.1029/2019JD031149, 2019.

Duan, J., Huang, R. J., Wang, Y., Xu, W., Zhong, H., Lin, C., Huang, W., Gu, Y., Ovadnevaite, J., Ceburnis, D., and O'Dowd, C.: Measurement report: Size-resolved secondary organic aerosol formation modulated by aerosol water uptake in wintertime haze, Atmos. Chem. Phys., 24, 7687–7698, https://doi.org/10.5194/acp-24-7687-2024, 2024.

Kim, N., Yum, S. S., Park, M., Park, J. S., Shin, H. J., and Ahn, J. Y.: Hygroscopicity of urban aerosols and its link to size-resolved chemical composition during spring and summer in Seoul, Korea, Atmos. Chem. Phys., 20, 11245–11262, https://doi.org/10.5194/acp-20-11245-2020, 2020.

Xu, W., Chen, C., Qiu, Y., Xie, C., Chen, Y., Ma, N., Xu, W., Fu, P., Wang, Z., Pan, X., Zhu, J., Ngcg, N. L., and Sun, Y.: Size-resolved characterization of organic aerosol in the North China Plain: New insights from high resolution spectral analysis, Environ. Sci. Atmos., 1, 346–358, https://doi.org/10.1039/d1ea00025j, 2021.

Xu, W., Kuang, Y., Xu, W., Zhang, Z., Luo, B., Zhang, X., Tao, J., Qiao, H., Liu, L., and Sun, Y.: Hygroscopic growth and activation changed submicron aerosol composition and properties in the North China Plain, Atmos. Chem. Phys., 24, 9387–9399, https://doi.org/10.5194/acp-24-9387-2024, 2024.

RC10. Line 228-229, Line 235-236 The two sentences are not consistent.

Response: We have revised the sentences:

L247-250: This could be largely attributed to the reduction in anthropogenic emissions (e.g., NO₂, CO, except SO₂) from limited outdoor activities influenced by the heatwaves in P2, as well as partly suspended industries and transportation to alleviate the power shortage issue (Chen et al., 2024).

RC11. Line 239-241 Are the mean values of 1.6 ± 0.1 and 1.7 ± 0.2 during the P1 and P2 periods different significantly?

Response: We have conducted a Welch's t-test to evaluate the significance of the difference between the f(RH) values during different periods. The results indicate that the difference is statistically significant (p < 0.05). We have adjusted the corresponding sentence:

L259-261: The f(RH) was found to be relatively higher (p < 0.05) in heatwave days, with the mean values of 1.61 ± 0.12 and 1.71 ± 0.15 during the P1 and P2 periods, respectively.

RC12. Line 241-243 Do you think the results is dependent on the algorithm of ALWC? Please clarify it.

Response: The method of calculating ALWC by using the humidified nephelometer system has been presented in the response to **RC7** (Referee #3), which suggests that ALWC is largely dependent on the difference in aerosol volume concentration (e.g., related with the aerosol loading) between the dry and humidified conditions. We have revised it as below:

L261-266: Differently, ALWC was more abundant during the normally hot P1 period than the heatwave-dominated P2 period. This is likely due to that the derivation algorithm of ALWC utilized in this study (Kuang et al., 2018) was partly dependent on (e.g., positively correlated) the dry aerosol scattering coefficient, or rather the aerosol volume concentration in the dry condition (refer to Sect. S3 and Fig. S11 of the supplement).

RC13. Line 278-279 relatively polluted?

RC1 of Referee#2 (Figure R1). The mean $\sigma_{sca, 525}$ and PM_{2.5} during P1 period were 113.6% and 49.5% higher than those for P2 period, respectively, and the mean visibility was 22.1% lower than that of P2 period. In addition, the mean CS of P1 NPF_P events is higher than 0.015 s⁻¹, which can be also identified as the polluted-type NPF day (Shang et al., 2023). We have revised the manuscript accordingly.

L310-315: As stated in Sect.3.1, NPF events during the P1 period tended to occur in relatively polluted environments compared to that of P2 NPF_C, HW events, as evidenced by the frequent occurrence of $\sigma_{sca, 525} > 100 \text{ Mm}^{-1}$, increased air pollutant concentrations and lower visibility levels during P1 (Table S2, Fig. 1). Additionally,

the mean CS of the NPF_P events was above 0.015 s⁻¹ (Table S2), which could be considered as the "polluted" NPF day (Shang et al., 2023).

Updates in the reference list:

Shang, D., Hu, M., Tang, L., Fang, X., Liu, Y., Wu, Y., Du, Z., Cai, X., Wu, Z., Lou, S., Hallquist, M., Guo, S., and Zhang, Y.: Significant effects of transport on nanoparticles during new particle formation events in the atmosphere of Beijing, Particulogy, 80, 1–10, https://doi.org/10.1016/j.partic.2022.12.006, 2023.

RC14. Line 284-285 the upper detection limit of 30 km? please clarify it

Response: Although no specific information on the upper limit of the visibility data used in this study (i.e., from the Integrated Surface Database (ISD)), long-term observations using the same visibility records consistently show values not exceeding 30 km (Mukherjee and Toohey, 2016; Xu et al., 2020; Zhao et al., 2022). To avoid unnecessary misleading, we have revised the sentence:

L317-319: In addition, the mean $PM_{2.5}$ concentration was even lower than $10.0 \,\mu\text{g}\cdot\text{m}^{-3}$, and the corresponding visibility level was almost maintained at 30 km (Fig. 1e).

RC15. Line 291-292 why the authors emphasize that "sulfuric acid concentration was a critical factor for the occurrence of P1 NPF events."? Do you mean P1 NPF and P2 NPF different? Figure2f show the diurnal variation of H₂SO₄ during different periods with minor difference.

Response: We thank the reviewer for raising this important question. NPF_P events typically occurred around 11:00 LT during the P1 period, and the H₂SO₄ (SO₂) concentration on NPF_P days was 5.3% (19.3%) higher than that on non-event days at this time. Although NPF_C, HW events occurred approximately one hour earlier during the P2 heatwave period, the corresponding H₂SO₄ (SO₂) concentration on non-event days was conversely higher. This likely suggests a minor role of H₂SO₄ (SO₂) concentration in the P2 NPF_C, HW events. As discussed in the responses to **RC10** (Referee #2) and **RC17** (Referee #3), the extremely high temperatures likely

suppressed nucleation and growth processes on the P2 non-event days, even when H₂SO₄ (SO₂) concentrations were elevated.

Moreover, the predominant precursor species responsible for NPF events may vary under heatwave weather, depending on the concentration/type of precursors in the environment (Ma et al., 2016; Wang et al., 2017). For instance, recent studies have found that heatwaves likely led to changes in the abundance of precursors such as VOCs from both anthropogenic and biogenic sources (Chen et al., 2024).

Given the above reasons, we suggest that sulfuric acid could be a more critical factor for the occurrence of NPF_P events during the P1 period, in comparison to the P2 heatwayes.

RC16. Line 296-297 This might suggest that meteorological factors might not be the predominant determining factor of NPF occurrence? In this study, the measurement period is so short, more caution should be paid to reach this conclusion.

Response: We appreciate the reviewer for the comment and have adjusted the expression to avoid arbitrary statement:

L330-332: This likely suggests that meteorological factors might not be the predominant determining factor of NPF occurrence during the heatwaves of 2022 summer in urban Chongqing,

RC17. Line 309-311 "...the occurrence and subsequent growth of NPF during non-event days...", the sentence should be clarified.

Response: This can refer to our response to **RC10** of Referee #2. The higher temperatures likely prevented nucleation processes from meeting the criteria for NPF events and hindered the subsequent growth of nucleation mode particles, even if the concentrations of SO₂ and H₂SO₄ were higher on the P2 non-event days. We have revised the sentence:

L345-348: Hence, the even higher temperature (e.g., T > 40 °C) likely suppressed the nucleation processes and the subsequent growth of nucleation mode particles on P2

RC18. Line 319 NPF could occur worldwide, what's the temperature threshold of NPF events?

Response: The occurrence of NPF depends on a complex interplay of factors, including precursor gas types/concentrations, meteorological conditions, and pre-existing aerosol loading (Kerminen et al., 2018; Kulmala et al., 2003). Hence, there is no specifically defined temperature threshold of NPF events, although which have been observed around the world throughout the years (Crumeyrolle; et al., 2023; Dada et al., 2017). Accordingly, we have revised the content:

L357-361: Since the sunrise and sunset time did not significantly vary within the study period (i.e., less than a half hour discrepancy), heatwaves likely provided more favorable conditions (e.g., enhanced volatile gaseous emissions, low RH; Bousiotis et al., 2021; Hamed et al., 2007; Wang et al., 2024) for the occurrence of NPF events in urban Chongqing.

Update in the reference list:

Hamed, A., Joutsensaari, J., Mikkonen, S., Sogacheva, L., Dal Maso, M., Kulmala, M., Cavalli, F., Fuzzi, S., Facchini, M. C., Decesari, S., Mircea, M., Lehtinen, K. E. J., and Laaksonen, A.: Nucleation and growth of new particles in Po Valley, Italy, Atmos. Chem. Phys., 7, 355–376, https://doi.org/10.5194/acp-7-355-2007, 2007.

RC19. Line 359-360 during P2 heatwave-dominated NPF events? The meaning is not clear.

Response: We have revised the corresponding expression:

L405-407: Both HBF and SAE on P2 NPF_{C, HW} days were significantly higher than that of P1 NPF_P cases (Fig. 3c, e), largely due to the smaller R_{eff} observed during heatwave-dominated period (Table S2).

RC20. The PVSDs in Figure S3 a2-c2 are strange above ~ 500 nm, why?

Response: Upon checking the original size distribution data, we found that this phenomenon could be attributed to the following two factors. Firstly, the number concentrations of particles above 500 nm are quite close to each other and generally lower than 500 #/cm³, while these large particles can significantly contribute to the particle volume concentration. Secondly, the SMPS has larger size intervals (i.e., fewer size bins) for particle sizes above 500 nm compared to smaller size ranges. Besides, a similar pattern was observed for the PVSDs above 500 nm during P2 non-event days (Figure R11). However, occasionally occurred extremely high volume concentrations could render this effect comparatively less noticeable.

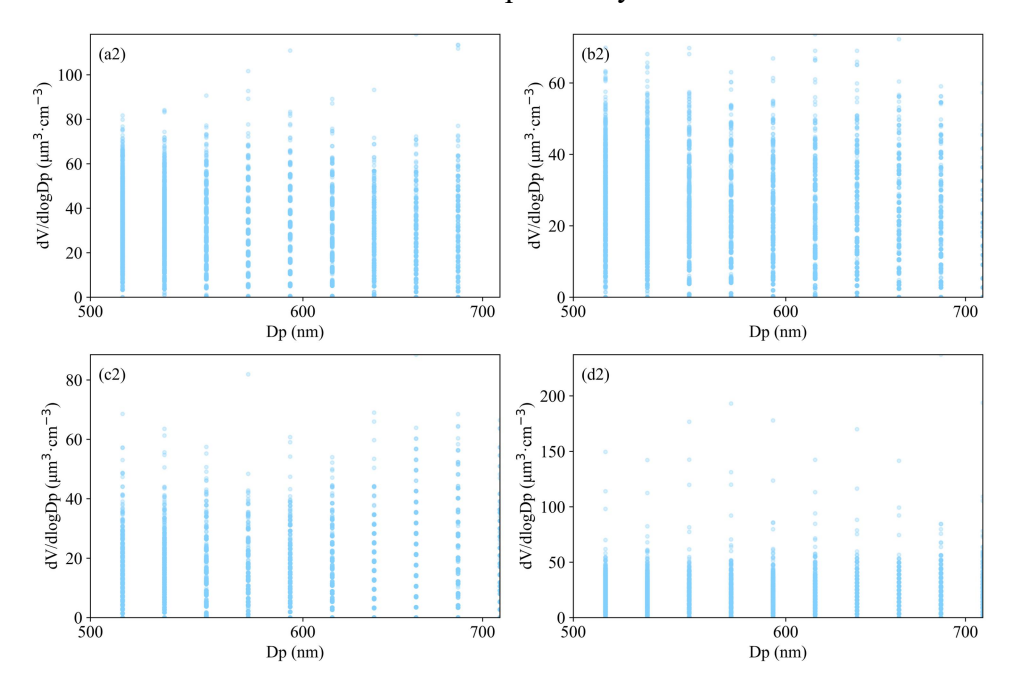


Figure R11. The PVSDs (a2-d2) of particles above 500 nm on P1 NPF event (a2) and non-event (b2) days, P2 NPF event (c2) and non-event (d2) days.

RC21. Section 3.3 Characteristics of the aerosol optical and hygroscopic properties during NPF events?

Line 338-339 What the meaning of NPF events in this study? Refer to the whole day?

Response: As clarified in our response to **RC1** of Referee #3, we have updated the section title to "3.3 Characteristics of the aerosol optical and hygroscopic properties on different types of NPF days". The mentioned time periods with "NPF events" have

been replaced with "NPF days", i.e., the whole day when NPF was observed, throughout the manuscript.

RC22. Line 403-405 This opinion could not supported by the data in Table S2, where the fw during P1 and P2 NPF are 0.47 ± 0.04 , 0.48 ± 0.05 , while 0.46 ± 0.04 and 0.46 ± 0.06 during P1 and P2 non-event days.

Response: We agree that the discrepancy in the corresponding mean f_W results is relatively insignificant, while the differences in the diurnal variations of f_W between NPF and non-event days were more pronounced. We have modified the content to highlight that during the subsequent growth and aging of pre-existing and new particles, the f_W of NPF days was higher than that of non-event days in the afternoon: **L448-453:** The f_W levels were slightly higher during NPF days in comparison to that of non-event days (Table S2). This difference was more pronounced in the afternoon of NPF days (e.g., even exceeded 50%; Fig. 3f), verified the enhancement of aerosol hygroscopicity during the subsequent growth and atmospheric aging of both pre-existing and newly formed particles.

RC23. Line 407-410, The authors mentioned "data mainly within the time window of 08:00-22:00 were utilized for the following discussion", but, Figure 4a and 4b included other data, please clarify it.

Response: The full diurnal patterns of NF_{Acc.} and VF_{Acc.} in Figure 4a and 4b were shown to illustrate the significant impact of NPF events and subsequent growth on aerosol size distributions, particularly in comparison to non-event days. We have highlighted the time window of 08:00-22:00 LT in Figure 4a and 4b to facilitate the corresponding discussion (see in **RC5** of Referee #2) and updated the manuscript accordingly.

L481-484: This is mainly due to the explosive formation of ultrafine particles and subsequent growth on NPF days, significantly altering aerosol size distributions and inducing large fluctuations in the number and volume fractions of accumulation mode particles (as shaded in Fig. 4a-b).

RC24. Why only a few data in Figure 4d is with the temperature above 40°C

Response: In fact, the high values of f(RH) (e.g., f(RH) > 1.7) generally corresponded to extremely high temperatures above 40 °C on P2 non-event days (see Figure R12 as below). During the heatwave-dominated P2 period, intensified photochemical reactions led to the formation of more hygroscopic secondary aerosols, which increased both R_{eff} and f(RH).

The few data points highlighted by the red dashed circle in Figure 4d were attempted to emphasize that even smaller particles ($R_{\rm eff}$ <110 nm) could exhibit high f(RH) levels under such extreme temperature conditions (T >40 °C). This likely highlights the significant impact of intense photochemical reactions on aerosol hygroscopicity during the heatwaves, particularly in comparison to P1 non-event days.

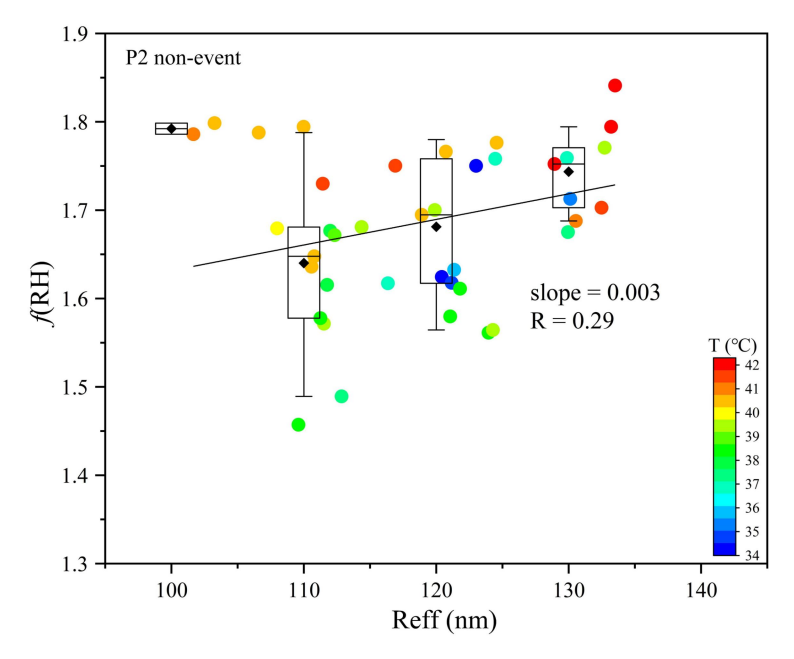


Figure R12. The relationship of f(RH) with R_{eff} and temperature (as indicated by the colored dots) on P2 non-event days.

RC25. Figure 5 Why the authors labeled polluted and relatively polluted in Figure 5a and 5b for P1 NPF and P2 NPF, respectively? which is not consistent "in clean environment" mentioned above in the manuscript?

Response: We appreciate the reviewer's attention to this inconsistency. In the original version, we intended to indicate that lower values of the SAE and f(RH) corresponded to higher scattering coefficients, reflecting higher aerosol loading conditions. To avoid unnecessary misunderstandings, we have removed the "polluted" and "relatively polluted" labels from Figure 5.

RC26. Line 447-449 Such a positive (negative) correlation of f(RH) with SAE (CS) was more pronounced in heatwave-induced high temperature days during P2 period. Which is not supported by the correlation R = 0.58 during P2 NPF in Figure 5b1, while R = 0.65 during P1 NPF in Figure 5a1.

Response: Thanks for pointing out this mistake. Upon re-examining the original data, we confirmed that the correlation coefficient between f(RH) and SAE during P1 NPF_P days (R = 0.65) is indeed higher than that during P2 NPF_{C, HW} days (R = 0.58). This may be attributed to the different NPF events during the P2 heatwave-dominated period, as detailed in our response to **RC2** (Referee #2). We have removed such erroneous conclusions from both Section 3.4 and the final conclusions section:

L498-500: Aerosol f(RH) and SAE exhibited a higher level on P2 $NPF_{C, HW}$ days (as shown by the dash lines in Fig. 5), the possible reasons can be attributed to the following two aspects.

L671-673: A significantly positive (negative) correlation between f(RH) and SAE (CS, $\sigma_{sca, 525}$, or rather the pollution level) was observed on NPF days for both periods, accompanied by higher f(RH) and SAE values on NPF_{C, HW} days.

RC27. Line 463-465 It is worth noting that f(RH) did not show a consistently higher level after the NPF occurrence during P2 period, and it was slightly higher within the first few hours of NPF occurrence during P1 NPF events (Fig. 3b). Which is hard to see from Figure 3b.

Response: As shown by the dashed circle in Figure R13, the f(RH) on P1 NPF_P days was higher than that on P2 NPF_{C, HW} days during the time period of ~ 12:00-15:00 LT (i.e., following the NPF occurrence).

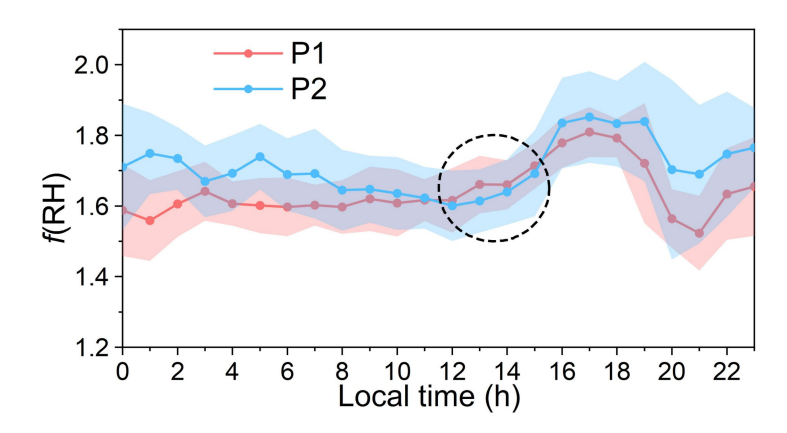


Figure R13. Diurnal variation f(RH) on NPF days during P1 (red line) and P2 (blue line) periods. The shaded areas stand for the corresponding $\pm 1\sigma$ standard deviations.

We have included the specific time period in the revised manuscript:

L514-515: and it was slightly higher within the first few hours of NPF occurrence (i.e., $\sim 12:00$ -15:00 LT) on P1 NPF_P days (Fig. 3b).

L683-685: further leading to a lower f(RH) following the NPF occurrence (i.e., \sim 12:00 -15:00 LT) in comparison to P1 NPF_P days.

RC28. Line 474-476 The critical sizes corresponding to the cumulative frequency of 50% in $\sigma_{sca, 525}$ were 358.7 nm and 333.8 nm on P1 and P2 NPF event days, respectively. Have you seen the particles grow to this particles during NPF events?

Response: The aerosol optical properties (e.g., light scattering) are inherent and influenced by their size distributions. The total aerosol scattering coefficient is predominantly influenced by larger particles, which are unnecessarily originate solely from the growth of newly formed particles. Instead, these larger particles could be resulted from the mixing of pre-existing particles with newly formed ones that may undergo subsequent growth and aging processes. Therefore, the observed critical sizes corresponding to the cumulative frequency of 50% in $\sigma_{sca, 525}$ (D₅₀) likely represent a combination of pre-existing and aged larger particles. Additionally, similar D₅₀ values were observed on non-event days, indicating that such size ranges are not exclusive to

NPF events. We have revised the sentences to highlight the contribution of the pre-existing and aged large particles:

L526-529: This indicates that relatively smaller particles including the newly formed and grown ones mixed with pre-existing and aged particles contributed a slightly higher portion to $\sigma_{sca, 525}$ on P2 NPF_{C, HW} days, while the $\sigma_{sca, 525}$ was mainly contributed by larger ones on P1 NPF_P days.

RC29. Line 485-486 "...leading to a reduced enhancement in aerosol light scattering...", please make it clear

Response: We have revised the sentence as below:

L534-537: Newly formed ultrafine particles contributed minor to aerosol optical properties, resulting in a lower f(RH) during the initial hours of P2 NPF_{C, HW} events compared to that of P1 NPF_P events (Fig. 3b), as evidenced by a smaller R_{eff} for P2 NPF_{C, HW} events (Fig. S6).

RC30. Line 540-542 It should be noted that the reported $f_{RF}(RH)$ for the UGR site (Spain) was even higher, likely due to the relatively larger HBF in that area (Titos et al., 2014; 2021). This is not supported by the data in black dots (black dots for urban sites, UGR is an Urban site) Figure 2 in Titos et al 2021, although it is really hard to see which black dot is for UGR.

Response: Upon re-examining the raw HBF data in Titos et al. (2014), we acknowledge that attributing the higher $f_{RF}(RH)$ in the UGR site to a larger HBF may not be fully justified, as the mean HBF (0.15) for UGR are comparable to that during P2 period (0.153) in this study. To clarify this discrepancy, we identified a key methodological difference: Titos et al. (2014) originally used a surface reflectance constant (R_S) of 0.15, consistent with the globally averaged value adopted in our and previous studies (Fierz-Schmidhauser et al., 2010; Xia et al., 2023; Zhang et al., 2015). However, in their 2021 study, the R_S was changed to 0.25 (for rural, urban and mountain sites), which likely contributed to the higher $f_{RF}(RH)$ values reported for the UGR site. If the constant R_S = 0.25 was used in the derivation of $f_{RF}(RH)$ in this study,

the mean $f_{RF}(RH)$ (nearly 2.5) on the P2 NPF_C, HW days would be higher than that in the UGR site. Other factors such as variations in the mass scattering efficiency (α_s) could also contribute to the observed differences. As Titos et al. (2020) mentioned, aerosol scattering was largely enhanced after water uptake in URG, suggesting that α_s was likely higher in the UGR site under the condition of similar f(RH) levels between the two sites.

We have revised the content in the manuscript:

L600-602: It should be noted that the reported $f_{RF}(RH)$ for the UGR site (Spain) was even higher, likely due to the higher R_s and α_s used in the derivation of $f_{RF}(RH)$ in that area (Titos et al., 2021).

RC31. Line 565-566 "the new particles of higher hygroscopicity could contribute more to the activation of CCN," this opinion is not supported by aerosol optical hygroscopicity measurement, however, could be supported by HTDMA hygroscopicity measurement.

Response: Thanks for the suggestion, and we have revised the content accordingly:

L624-629: On the other hand, a large number of studies have demonstrated that the new particles of higher hygroscopicity could contribute more to the activation of CCN (Ma et al., 2016; Ren et al., 2021; Rosati et al., 2022; Sun et al., 2024; Wu et al., 2015), thereby modulating the aerosol-cloud interactions and further the global climate (Fan et al., 2016; Merikanto et al., 2006; Westervelt et al., 2013).

Updates in the reference list:

Fan, J., Wang, Y., Rosenfeld, D., and Liu, X.: Review of aerosol-cloud interactions: Mechanisms, significance, and challenges, J. Atmos. Sci., 73, 4221–4252, https://doi.org/10.1175/JAS-D-16-0037.1, 2016.

Merikanto, J., Spracklen, D. V, Mann, G. W., Pickering, S. J., and Carslaw, K. S.: Atmospheric Chemistry and Physics Impact of nucleation on global CCN, Atmos. Chem. Phys, 9, 8601–8616, 2009.

Rosati, B., Isokääntä, S., Christiansen, S., Jensen, M. M., Moosakutty, S. P., De Jonge,

R. W., Massling, A., Glasius, M., Elm, J., Virtanen, A., and Bilde, M.: Hygroscopicity and CCN potential of DMS-derived aerosol particles, Atmos. Chem. Phys., 22, 13449–13466, https://doi.org/10.5194/acp-22-13449-2022, 2022.

Westervelt, D. M., Pierce, J. R., Riipinen, I., Trivitayanurak, W., Hamed, A., Kulmala, M., Laaksonen, A., Decesari, S., and Adams, P. J.: Formation and growth of nucleated particles into cloud condensation nuclei: Model-measurement comparison, Atmos. Chem. Phys., 13, 7645–7663, https://doi.org/10.5194/acp-13-7645-2013, 2013.

RC32. Figure S8, It seems the fitting equation wrong.

Response: Thank you for pointing out this mistake, and we have corrected the fitting equation.

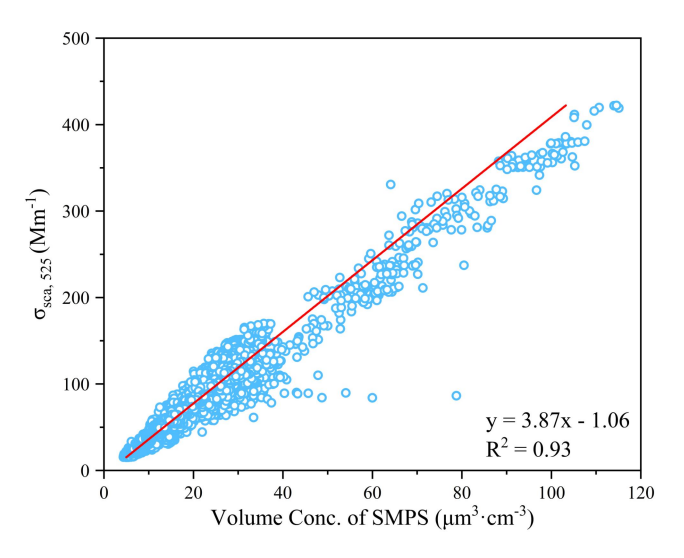


Figure S11. Correlation between the particle volume concentration determined by SMPS and $\sigma_{sca, 525}$ measured by the humidified nephelometer system during the study period. The solid line represents the fitting line.

Reference

Mukherjee, A. and Toohey, D. W.: A study of aerosol properties based on observations of particulate matter from the U.S. Embassy in Beijing, China, Earth's Futur., 4, 381–395, https://doi.org/10.1002/2016EF000367, 2016.

Pinnick, R. G., Jennings, S. G., and Ch, P.: Relationships Between Extinction, Absorption, Backscattering, and Mass Content of Sulfuric Acid Aerosols, J. Geophys. Res., 85, 4059–4066, 1980.

Titos, G., Lyamani, H., Cazorla, A., Sorribas, M., Foyo-Moreno, I., Wiedensohler, A., and Alados-Arboledas, L.: Study of the relative humidity dependence of aerosol light-scattering in southern Spain, Tellus, Ser. B Chem. Phys. Meteorol., 66, https://doi.org/10.3402/tellusb.v66.24536, 2014.

Xu, W., Kuang, Y., Bian, Y., Liu, L., Li, F., Wang, Y., Xue, B., Luo, B., Huang, S., Yuan, B., Zhao, P., and Shao, M.: Current Challenges in Visibility Improvement in Southern China, Environ. Sci. Technol. Lett., 7, 395–401, https://doi.org/10.1021/acs.estlett.0c00274, 2020.

Zhao, G., Hu, M., Zhang, Z., Tang, L., Shang, D., Ren, J., Meng, X., Zhang, Y., Feng, M., Luo, Y., Yang, S., Tan, Q., Song, D., Guo, S., Wu, Z., Zeng, L., Zhang, Y., and Xie, S.: Current Challenges in Visibility Improvement in Sichuan Basin, Geophys. Res. Lett., 49, https://doi.org/10.1029/2022GL098836, 2022.